

A fuzzy adaptive evolutionary-based feature selection and machine learning framework for single and multi-objective body fat prediction

Farshid Keivanian¹

Farshid.Keivanian@uon.edu.au

Raymond Chiong¹

Raymond.Chiong@newcastle.edu.au

Zongwen Fan²

Zongwen.Fan@hqu.edu.cn

¹School of Information and Physical Sciences, The University of Newcastle, Callaghan, Australia

²College of Computer Science and Technology, Huaqiao University, Xiamen 361021, China

Abstract

A well-performed body fat prediction can provide medical practitioners and users with essential information for appropriate decision-making in preventing and diagnosing heart diseases and premature deaths. By selecting the most relevant (vital) body measurements and capturing complex nonlinear relationships among selected features, hybrid machine learning models have been demonstrated to offer better performance than simple regression analysis methods in modelling body fat prediction problems. There are, however, some disadvantages to them. Current machine learning models often get stuck in local optima when modelling body fat prediction as a combinatorial single- and multi-objective optimisation problem using large datasets. Avoiding local optima becomes more challenging when multiple feature subsets produce similar or close predictions. Several machine-learning-based optimisation problems have been solved using evolutionary feature selection as an exploratory-exploitative metaheuristic algorithm. Fuzzy set theory determines appropriate levels of exploration and exploitation while managing parameterisation and computational costs by converting descriptive convergence status into fuzzy rules. We first explored a weighted-sum body fat prediction approach using evolutionary feature selection, fuzzy set theory, and machine learning algorithms, and integrating contradictory metrics into a single composite goal optimised with fuzzy adaptive evolutionary feature selection-based search strategies. This single-objective body fat prediction problem is addressed by a hybrid fuzzy adaptive global learning local search universal diversity-based feature selection-machine learning framework (FAGLSUD-based FS-ML). Compared to other hybrid and state-of-the-art machine learning models, this model achieved a more accurate and stable estimate of body fat percentage while using fewer features. A multi-objective FAGLSUD-based FS-MLP is also proposed to simultaneously analyse the conflicts between accuracy, stability, and dimensionality. Medical practitioners and users can use a well-distributed global optimal Pareto set of trade-off solutions to make informed decisions about fat deposits in the most vital body parts and blood lipid levels.

Keywords: *Body fat prediction; evolutionary computation-based feature selection; fuzzy logic theory; multi-objective optimisation; multimodality; parameterisation*

1. INTRODUCTION

In the past decade, nearly 100 million healthy life-years have been lost to diseases such as heart disease, diabetes, strokes, lung cancer, and chronic obstructive pulmonary disease (WHO, 2020). The global cost of heart diseases is expected to rise from US\$863 billion in 2010 to US\$1,044

billion by 2030. Cardiovascular Risk Factors (CRFs) are used by healthcare professionals to estimate the likelihood of heart attacks. A high percentage of body fat (PBF) is associated with CRF (Saito, Takahashi, Arioka, & Kobayashi, 2017), which can be used to detect CRF accumulation early. In order to assess the CRF and prevent serious diseases and high healthcare costs, it is crucial to predict body fat.

Several studies treated body fat prediction as an optimisation problem using simple regression analysis, and the best solution was found by searching in one direction based on the exact search strategy using anthropometric data (weight, height, waist circumference) (Deurenberg, Yap, & Van Staveren, 1998; Freedman, Dietz, Srinivasan, & Berenson, 2009; Johnson, 1996a; Sakai, Demura, & Fujii, 2009; Svendsen, Haarbo, Heitmann, Gotfredsen, & Christiansen, 1991). This technique has several advantages, including portability, noninvasiveness, affordability, and applicability in field studies (Wang, Thornton, Kolesnik, & Pierson Jr, 2000). Simple regression analysis, however, assumes that data structures are generated linearly, so complex and nonlinear data structures cannot be modelled. By capturing complex nonlinear relationships between variables, hybrid artificial intelligence algorithms can model body fat prediction problems more effectively than simple regression analysis algorithms (DeGregory et al., 2018; Hussain, Cavus, & Sekeroglu, 2021; Safaei, Sundararajan, Driss, Boulila, & Shapi'i, 2021; Shao, 2014). To predict PBF, Fan, Chiong, Hu, Keivanian, and Chiong (2022) proposed an intelligent hybrid approach in two stages. After obtaining fewer but more critical measurement variables in the first stage, those variables served as inputs into four machine learning methods—MLP, SVM, Random Forest, and eXtreme Gradient Boosting to predict PBF in the second stage. Using two benchmark body fat datasets (hereafter Johnson: 252 individuals, each with 13 features, and NHANES: 862 individuals, each with 41 features), a hybrid factor analysis-XGBoost (FA-XGBoost) model with superior accuracy was compared to hybrid and standalone models.

Evolutionary computation methods such as genetic algorithms (Ghareb, Bakar, & Hamdan, 2016; Jiang, Chin, Wang, Qu, & Tsui, 2017; Sikora & Piramuthu, 2007), differential evolution (He, Zhang, Sun, & Dong, 2009), particle swarm optimisation (Cervante, Xue, Zhang, & Shang, 2012; Gunasundari, Janakiraman, & Meenambal, 2016; Lin, Ying, Chen, & Lee, 2008), ant colony optimisation (Ghasab, Khamis, Mohammad, & Fariman, 2015; Goodarzi, Freitas, & Jensen, 2009), and imperialist competitive algorithm (Mirhosseini & Nezamabadi-pour, 2018) have been successfully applied as a search strategy for feature selection before training a machine learning model, which is a significant pre-processing operation of data mining. They generate multiple candidate feature subset solutions through global and local search capabilities, which are then fed into machine learning algorithms. Due to this, they have an advantage in terms of global and local searchability, which maintains the diversity of the population and makes computing more efficient. The use of multi-objective evolutionary computation-based feature selection-machine learning techniques facilitates the assessment of trade-offs between conflict objectives. Typically, they focus on improving accuracy and reducing dimensionality. A non-dominated sorting genetic algorithm-II (NSGA-II)-probabilistic neural network model is an example (Soyel, Tekguc, & Demirel, 2011) minimises the number of features and maximises the accuracy. Multi-objective particle swarm optimisation (MOPSO)-K-nearest neighbour model (Xue, Zhang, & Browne, 2014) reduces the number of features and accuracy.

Body Fat Prediction (BFP) was shown to be an NP-hard combinatorial optimisation problem (Keivanian, Chiong, & Hu, 2019). As far as we know, multi-objective evolutionary feature selection-based machine learning models have yet to be used to predict body fat. As a result, we will fill a research gap in single-objective and multi-objective BFP problems by reducing the number of predictors (nf), the accuracy (RMSE), and the stability (STD). Multiple feature subsets in the search domain produce similar or close predictions, known as multimodality complexity. This becomes more challenging for high-dimensional search spaces (13-dimensional and 41-dimensional search domains for Johnson and NHANES datasets, respectively). In order for single-

objective and multi-objective evolutionary feature selection to be accurate and efficient, the parameters must be set appropriately. As a result, parameterisation and computational cost issues arise, requiring the right exploration and exploitation level. Two recently proposed evolutionary feature selection-based body fat–predicting approaches developed fuzzy inference systems (FISs) that use fuzzy set theory (Zadeh, 1978) to transform descriptive convergence status into fuzzy rules that assist in determining the appropriate level of exploration and exploitation while observing and managing parameter uncertainties. The fuzzy adaptive binary genetic algorithm-based feature selection-MLP (FABGA-based FS-MLP) incorporates a FIS for adapting the parameters of GA's binary operators (i.e., crossover and mutation) (Farshid Keivanian & Nasser Mehrshad, 2015). The fuzzy adaptive global learning imperialistic competitive algorithm-based feature selection-MLP (FA-GL-BICA-based FS-MLP) incorporates two FISs: one for adapting the parameters of operators and another for selecting operators according to their contribution to the search in the past (Farshid Keivanian et al., 2019). Based on simulation results, the latter approach was slightly more accurate than hybrid machine learning and evolutionary feature selection. However, both methods were demonstrated only on the study's benchmark body fat dataset (Johnson dataset) (Johnson, 1996a). Furthermore, both approaches aim to find the best balance between accuracy and dimensionality without considering predictive stability. A satisfactory balance between accuracy, stability, and the number of selected features, i.e., multi-objectivity, must also be maintained.

Our study uses two sophisticated approaches to predict body fat: fuzzy adaptive global learning local search universal diversity-based feature selection-MLP (FAGLSUD-based FS-MLP) for predicting PBF at low *nf*, low RMSE, and low STD, and multi-objective FAGLSUD-based FS-MLP to analyse conflicts between *nf*, RMSE, and STD objectives simultaneously. The proposed fuzzy adaptive evolutionary feature selection strategy extends the subpopulation-based search strategies and fuzzy inference rules of the recently proposed single and multi-objective fuzzy adaptive enhanced imperialist competitive algorithms (FAEICA and MOFAEICA) (Keivanian & Chiong, 2022). This study solved multimodal (i.e., multiple local optima) single-objective and multi-objective optimisation problems of varying dimensions. An adaptive velocity limit function (AVLF) is designed to allow high exploration at an early stage of evolutionary feature selection and high exploitation at a later stage. We are motivated to boost evolutionary feature selection's exploration, exploitation, and information-sharing capabilities, to avoid premature convergence when locating the optimal set of features. A FAGLSUD-based FS-MLP provided an excellent balance between low *nf*, RMSE, and STD. Fuzzy logic theory's ability to adapt and select operators eliminates the need for parameter setting. It was shown that the FAGLSUD-based FS-MLP framework could provide medical practitioners and users with a more accurate and stable, and less dimensional estimation of PBF than several hybrid machine learning models and state-of-the-art evolutionary computation-based FS-machine learning models. MOFAGLSUD-based FS-MLP extends FAGLSUD-based FS-MLP by incorporating a diversity-aware index based on the central moment concept, known as spatial spread deviation, associated with ranking (SSDR), which helps identify a well-distributed set of trade-offs in the objective space and promotes diversity of solutions in the decision space to prevent premature convergence. As a result of this multi-objective approach, medical practitioners and users can make informed decisions based on their preferences regarding the measured fat deposits across the most vital body parts by generating a well-distributed global optimal Pareto set of low-dimensional-accurate-stable trade-off solutions.

Following is a summary of the remainder of this paper. The formulation of single-objective and multi-objective body fat prediction problems and their complexities are discussed in Section 2. The framework is presented in Section 3. Experiments, results, and discussion are presented in Section 4. We conclude our study in Section 5, point out its limitations, and outline potential future research plans.

2. SINGLE-OBJECTIVE AND MULTI-OBJECTIVE BODY FAT PREDICTION PROBLEM

A single-objective and multi-objective body fat prediction problem (SOBFP and MOBFP) is defined in this section (see sections 2.1 and 2.2), followed by an explanation of the objective functions that must be optimised in both problems in order to estimate the body fat percentage with the greatest accuracy (i.e., low RMSE), stability (i.e., low STD), and dimensionality level (i.e., low n_f). Then, we show that these three objectives are indeed in conflict and hold a strong Pareto relation (see Sections 2.2 and 4.6). Section 2.3 represents the design variables. Taking all objective function values into account simultaneously, no solution is better than the other when considering all Pareto-optimal body fat predictions with different degrees of accuracy, stability, and dimensionality. Section 2.4 illustrates multimodality complexity, where multiple solutions in decision space have similar objective functions in objective space, resulting in premature convergence. To deal with multimodality issues in MOBFP, section 2.5 introduces the central moment concept. SOBFP and MOBFP problems can be solved using FAGLSUD-based FS-MLP and MOFAGLSUD-based FS-MLP (see Sections 3 and 4).

2.1. SOBFP

Single-objective body fat prediction (SOBFP) is the process of optimising a linear combination of dimensionality, accuracy, and stability:

$$Z(\bar{X}_s) = \sum_{i=1}^M W_i O_i, \quad \sum_{i=1}^M W_i = 1, \quad W_i > 0, \quad M = 3 \quad (1)$$

Mathematical analysis is conducted to find appropriate relations between the weights. In theory, $\frac{W_1}{W_2}$ is proportional to $RMSE$ as $\frac{W_1}{W_2} = \beta \cdot RMSE$. An empirical study is carried out to assign optimum values to each weight. According to our previous studies (F Keivanian & N Mehrshad, 2015), (F Keivanian, R Chiong, & Z Hu, 2019), the best value for β is 0.04.

$$O_i(\bar{X}_s) = \begin{cases} O_1: \min f_1 = n_f \\ O_2: \min f_2 = RMSE(t, f) \\ O_3: \min f_3 = STD(error) \end{cases} \quad (2)$$

$$RMSE = \sqrt{\frac{1}{N_{Total}} \times \sum_{i=1}^{N_{Total}} (t_i - f_i)^2} = \sqrt{\frac{1}{N_{Total}} \times \sum_{i=1}^{N_{Total}} (e_i)^2} \quad (3)$$

$$STD = \sqrt{\frac{1}{N_{Total}} \sum_{i=1}^{N_{Total}} (e_i - \mu)^2} \quad (4)$$

$$\mu = E(e) = \frac{1}{N_{Total}} \sum_{i=1}^{N_{Total}} e_i \quad (5)$$

where N_{Total} is the total number of observations (i.e., data samples), t_i is to the target value, f_i is the prediction value achieved by the approach, n_f is the size of selected features, μ or E is the expectation (e) of the prediction and \bar{X}_s is the feature subset found by the framework.

$$Z(\bar{X}_s) = W_1 n_f + W_2 RMSE + W_3 STD \xrightarrow{\div W_2} Z = \frac{W_1}{W_2} n_f + RMSE + \frac{W_3}{W_2} STD \quad (6)$$

$$Z(\bar{X}_s) = RMSE(1 + \beta \cdot n_f) + \gamma \cdot STD \quad (7)$$

If $r_f = \frac{n_f}{n_x}$, then $n_f = n_x \times r_f$, and $\gamma = \beta = 0.04$:

$$Z(\bar{X}_s) = RMSE(1 + 0.04 \times n_x \times r_f) + \gamma \cdot STD = RMSE(1 + 0.04 \times n_x \times r_f) + 0.04 \times STD \quad (8)$$

$$Power_{Sol,i} = Fitness_{Sol,i} = \frac{1}{Z(\overline{X}_{S_{Sol,i}})} = \frac{1}{RMSE_i(1+0.52 \times r_{f,i}) + 0.04 \times STD_i} \quad (9)$$

where n_x is the total number of features in the given dataset and r_f is the ratio of selected features. Our proposed method minimises $Z(\overline{X}_s)$ in each iteration, addressing minimisation of dimensionality, RMSE and STD in each run, and is able to find an optimal feature subset \overline{X}_s . Through the evolution process, Eq. (9) measures the fitness of each candidate feature subset.

2.2. MOBFP

Multi-objective body fat prediction problem (MOBFP) is the process of optimising each individual objective simultaneously without the need for scalarisation:

$$\bar{O}(\overline{X}_s) = [O_1(\overline{X}_s), O_2(\overline{X}_s), O_3(\overline{X}_s)] = [n_f, RMSE, STD] \quad (10)$$

In the context of the SOBFP and MOBFP problems, Johnson and NHANES are considered as thirteen and forty-one design variables, respectively.

2.3. Design variables

The proposed SOBFP and MOBFP problems involve 13 and 41 design variables with the following upper and lower search bounds, as shown in the following:

Benchmark dataset	Design variables	Lower bound (Var_{min})	Upper bound (Var_{max})
Johnson	$\overline{X}_s = [x_{s_1}, x_{s_2}, \dots, x_{s_{13}}]^T$	0	1
NHANES	$\overline{Y}_s = [y_{s_1}, y_{s_2}, \dots, y_{s_{41}}]^T$	0	1

Johnson is a collection of body experiments (demographic data: age; anthropometric data: weight and height; and ten body circumference measurements: neck, chest, abdomen, hip, thigh, knee, ankle, biceps, forearm and wrist), which NHANES is a collection of 36 types of physical examination, dietary and laboratory data, age group data (children, youth, adults, seniors), three basic types of anthropometric data (weight, height, waist circumference), and one questionnaire concentrating on anamnesis and lifestyle data (full sample two-year Mobile Examination Centre (MEC) exam weight).

2.4. Multimodality complexity

Multimodality properties indicate that multiple optimisation solutions in the decision space correspond to the same or similar optimisation results in the objective space. Both multimodal single-objective optimisation (MSOP) and multimodal multi-objective optimisation (MMOP) share this property. As MMOPs and MSOPs cause many local optima during the optimisation process, they are more challenging than general MOPs and SOPs.

Fig. 1 conceptually visualises the multimodal complexity of the body fat prediction problem. An approach of choice is the NSGA-II- (Deb, Pratap, Agarwal, & Meyarivan, 2002) based FS-MLP, which finds the local Pareto Sets (PSs) so close to one another in the decision space, corresponding to the local Pareto Fronts (PFs) close to one another in the objective space. Representative PSs are X_{s1} (x5: chest, x7: hip, x12: forearm), X_{s2} (x5: chest, x7: hip, x13: wrist), X_{s8} (x1: age, x2: weight, x3: height, x4: neck, x6: abdomen, x8: thigh, x9: knee, x10: ankle, x11: biceps, x13: biceps), X_{s9} (x1: age, x2: weight, x3: height, x4: neck, x6: abdomen, x8: thigh, x9: knee, x10: ankle, x11: biceps, x12: forearm) and X_{s10} (x1: age, x2: weight, x3: height, x4: neck, x6: abdomen, x7: hip, x9:

knee, x10: ankle, x11: biceps, x12: forearm). Their corresponding PFs comprise $F(X_{s1})$, $F(X_{s2})$, $F(X_{s8})$, $F(X_{s9})$ and $F(X_{s10})$.

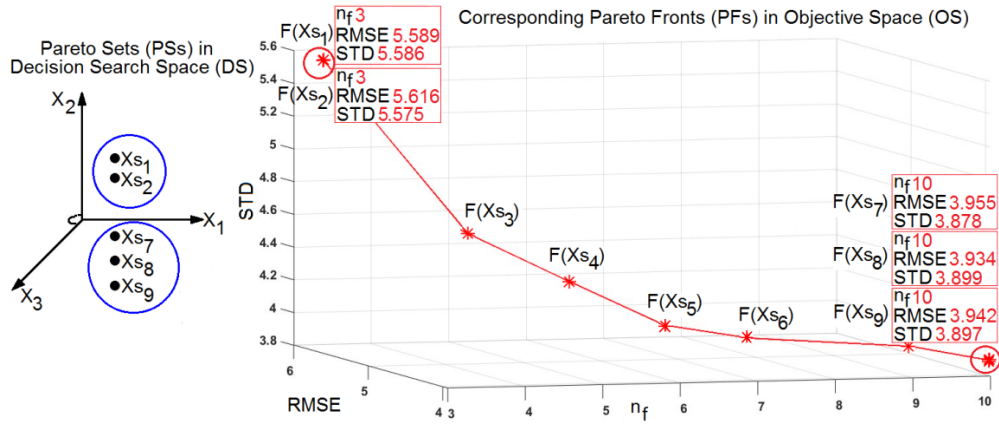


Fig. 1: A conceptual visualisation of the multimodal property of the body fat prediction problem

Liu, Yen, and Gong (2018) evaluated multi-objective evolutionary computation algorithm (MOECA)'s performance on multimodal multi-objective optimisation (MMOP) benchmarks and revealed that local PSs that correspond to PFs close to one another may cause inferior objectives surrounding a similar region. Accordingly, finding all local Pareto feature subset solutions that correspond to Pareto prediction results close to one another may not be interesting for body fat experts. Our focus here is on only finding all equivalent global and well-diversified PSs in the decision space associated with evenly distributed PFs in the objective space while avoiding becoming trapped in useless local optimal solutions. Thus, to deal with body fat prediction from the MMOP point of view, we will extend MOFAEICA (Keivanian & Chiong, 2022) which was shown with more promising results than salient MOECAs, such as NSGA-II (Deb et al., 2002), MOPSO (Coello, Pulido, & Lechuga, 2004), and multi-objective imperialist competitive algorithm (MOICA) (Enayatifar, Yousefi, Abdullah, & Darus, 2013) in terms of convergence and diversity metrics for two- and three-objective MMOPs.

2.5. Central moment concept

A central moment measures a random variable's expectation around a fixed value. In an M-dimensional objective space, consider the distance between optimisation results as a set of variables. By subtracting the expectations of these variables from their means, a well-distributed set of trade-off results can be identified. In Eq. (11), the moment (μ_n) is defined as a measure of discrete variables' shape.

$$\mu_n = \sum_{i=1}^{\infty} (x_i - c)^n p(x_i) \quad (11)$$

In this relation, x_i is one of the possible values for the random variable, $p(x_i)$ is its probability, n is its order, and c is its reference point. Different definitions of moments exist, such as raw moments and central moments. As $c = 0$, the raw moment is also called the absolute moment or the moment of a function. In statistics, the central moment is used to measure central tendency. The central moment replaces the value of c with the expected value or arithmetic mean \bar{x} . With an order of 2, it is easy to argue that the variance is the central moment for n points:

$$\mu_2 = \frac{1}{n} \sum_{i=1}^n (x_i - \bar{x})^2 \quad (12)$$

Variance can be calculated independently of probability density functions using Eq. (12). In the same way that sample means, and sample central moments are estimated from n samples without

knowing the probability density function, sample moments are estimates of the moments. Many observations will have a sample mean that is close to the expected value (a raw moment in the origin of order 1). Euclidean distances between pairs of data points in the objective space can be normalised. As a reference, we will use the difference between the maximum and minimum distance between points in this study. By minimising the moment of order 2 to this reference, the distances between points become equidistant, leading to a Pareto front approximation with a good distribution.

3. PROPOSED FRAMEWORK

This section explains the proposed framework and its multi-objective extended version.

3.1. Fuzzy adaptive global learning local search universal diversity-based feature selection-MLP (FAGLSUD-based FS-MLP)

This section describes the novel search components. An overview of the framework is shown in Fig. 2. Among the search components guided by FISs are fuzzy adaptive global learning-based velocity adaptation (FAGLVA), fuzzy adaptive universal diversity-based velocity divergence (FAUDVD), fuzzy adaptive enhanced differential evolutionary-based local search (FAEDELS), and fuzzy adaptive operator selection (FAOS). In the SOBFP problem, FAGLSUD-based feature selection extends FAEICA's search capabilities (Keivanian & Chiong, 2022). Their populations are divided into empires, which are subpopulations. A high-fitness solution - imperialism - and a low-fitness solution - colonies, which share information through interactions - exist. In contrast to other evolutionary computation techniques, this type of search trajectory has led to the development of numerous sub-individual search strategies for subdivided cooperative populations (Alixandre & Dorn, 2017; Gonçalves & Resende, 2011; Khaled & Hosseini, 2015; Roque, Fontes, & Fontes, 2014).

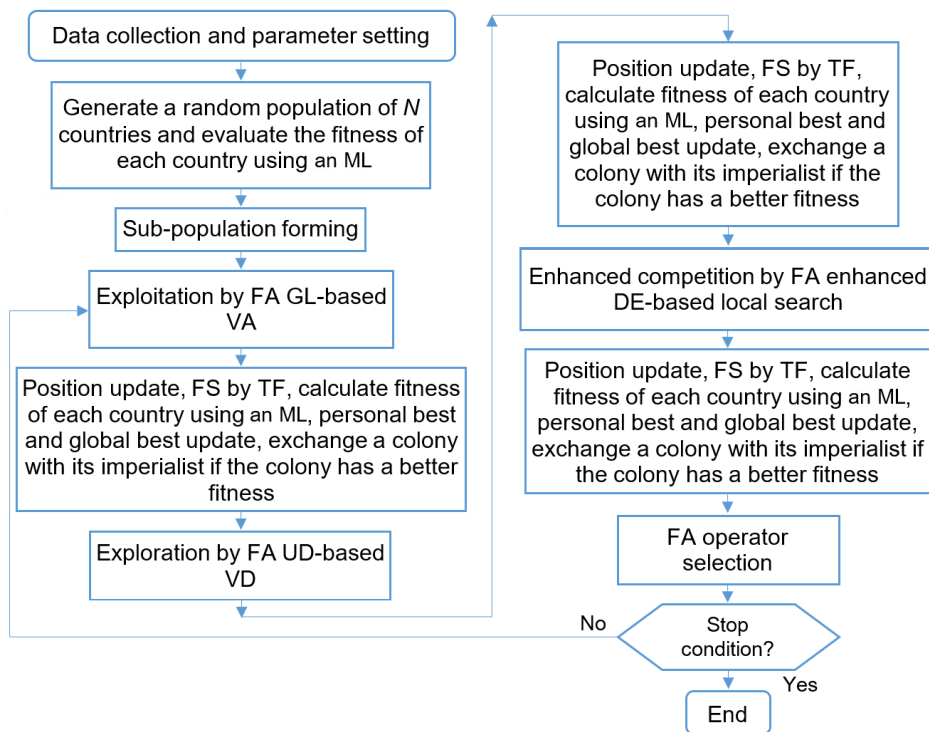


Fig. 2: The proposed FAGLSUD-based FS-ML

FAEICA's fuzzy adaptive global learning could only benefit colonies. In contrast, FAGLSUD's FAGLVA strategy targets colonies and imperialists. The colony learns from its associative

imperialists and local best experiences, and the imperialist learns from its global and best experiences. Thus, high-dimensional optimisation and prediction problems can be solved more efficiently and effectively. Fuzzy adaptive global best diversity strategy was only meant to update global best solutions. In contrast, FAGLSUD's FAUDVD learning mechanism facilitates the following: Each candidate colony learns from the best-known experience of other colonies. Imperialists learn from each other's best experiences. Furthermore, the best global imperialist learns from other imperialists' best-ever experiences. These learnings discourage premature convergence. A randomly selected colony can be moved towards its imperialist and in the reversed path of the worst colony by FAEICA's differential evolution-based local search. As well, FAGLSUD's FAEDEL models a randomly chosen imperialist direction toward the global best imperialist and in a reversed direction towards the worst imperialist. The framework is able to locate more optimal solutions as a result of these movements. FAGLSUD allows operators to be adapted and selected (FAOS) more purposefully to find global optimum solutions. A velocity limit function (AVLF) allows for a high exploration rate at an early stage of optimisation and a high exploitation rate at a later stage.

3.1.1. Adaptive velocity limit function (AVLF)

An interesting study by Azad and Hasançebi (2013) formulated an upper bound strategy that considers the current best design as the upper bound for the forthcoming candidates to eliminate unnecessary structural analysis and associated fitness computations for those candidates that have no chance of surpassing the best solution. For the SOBFP problem, an adaptive velocity limit function (AVLF) is defined to save the convergence time, as per the following relation:

$$\begin{cases} \overline{Vel}_{max} = +\alpha \left(\frac{Var_{max} - Var_{min}}{Var_{max}} \right) \times \left| \frac{P_{Globalbest}^t - P_{Sol,i}^t}{t} \right|, \forall \overline{P}_{Sol,i}^t \neq \overline{P}_{Globalbest}^t \\ \overline{Vel}_{max} = 0, \forall \overline{P}_{Sol,i}^t = \overline{P}_{Globalbest}^t \\ \overline{Vel}_{min} = -\overline{Vel}_{max} \\ \overline{Vel}_{min} < \overline{V}_{Sol,i}^t = [V_1, \dots, V_{nVar}] < \overline{Vel}_{max} \end{cases} \quad (13)$$

AVLF linearly decreases by the number of iterations, giving the current search location \overline{P}_{Sol}^t a tendency to keep moving toward the global best solution, $\overline{P}_{Globalbest}^t$ using fewer computational resources. AVLF enables a high exploration during the early stage of SOBFP process and high exploitation at the later stage of the SOBFP process. Herein, α was set to 10 based on the empirical study of several values.

3.1.2. Fuzzy adaptive global learning velocity adaptation (FAGLVA)

Fig. 3 shows a candidate solution in a sample two-dimensional decision space that shares information with its best-known experience, its local imperialist and the global best imperialist.

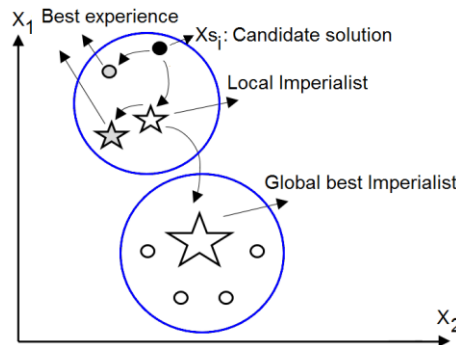


Fig. 3: Two-dimensional representation of FAGLVA's proposed search mechanism

$$\begin{cases} \overline{V_{Col,i}^{t+1}} = \beta_1 r_1 (\overline{P_{Imp,j}^t} - \overline{P_{Col,i}^t}) + c_1 r_2 (\overline{P_{lbestCol,i}^t} - \overline{P_{Col,i}^t}) \\ \overline{V_{Imp,j}^{t+1}} = \beta_2 r_1 (\overline{P_{Globalbest}^t} - \overline{P_{Imp,j}^t}) + c_2 r_2 (\overline{P_{lbestImp,j}^t} - \overline{P_{Imp,j}^t}) \end{cases}, \text{ if } r \leq PFAGLVA \quad (14)$$

where β_1, β_2 accelerate the learning process for colony i and imperialist j and $PFAGLVA$ is the probability of using the FAGLVA operator. Our proposed FAOS will determine $PFAGLVA$. If the evolved velocity vectors lie outside the search boundary of between Vel_{min} and Vel_{max} , the maximum and minimum values will be assigned to them. Then position component of each colony and imperialist updates as follows:

$$\begin{cases} \overline{P_{Col,i}^{t+1}} = \overline{P_{Col,i}^t} + \overline{V_{Col,i}^{t+1}} \\ \overline{P_{Imp,j}^{t+1}} = \overline{P_{Imp,j}^t} + \overline{V_{Imp,j}^{t+1}} \end{cases} \quad (15)$$

If the updated positions lie outside their search boundary Var_{min} to Var_{max} , the maximum and minimum values will be assigned to them and their corresponding velocities will be in reversed direction, multiplying by minus one. Eq. (16) measures the position changes over the iteration time:

$$u_n^d = \begin{cases} \Delta(P_{Col,i}^{t+1,d}) = V_{Col,i}^{t+1,d} \\ \Delta(P_{Imp,j}^{t+1,d}) = V_{Imp,j}^{t+1,d} \end{cases} \quad (16)$$

Eq. (17) maps evolved solutions obtained by the FAGLVA from the continuous decision space to the discrete binary decision space:

$$TF(u_n^d) = 2 \times \left| \frac{1}{1+e^{-8 \times u_n^d}} - 0.5 \right| \quad (17)$$

Fig. 4 illustrates the proposed TF. Eq. (18) applies our TF. Fig. 5 shows a transformation of the evolved Johnson feature subsets to the discrete binary decision space.

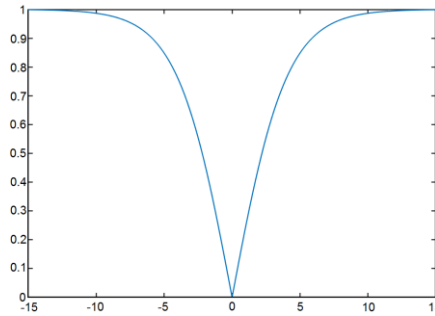


Fig. 4: The proposed V-shaped TF

$$\begin{cases} X_{Col,i}^{t+1,d} = \begin{cases} \text{Not}(X_{Col,i}^t) & \text{if } \text{rand}() < TF(\Delta(P_{Col,i}^{t+1,d})) \\ X_{Col,i}^t & \text{Otherwise} \end{cases} \\ X_{Imp,j}^{t+1,d} = \begin{cases} \text{Not}(X_{Imp,j}^t) & \text{if } \text{rand}() < TF(\Delta(P_{Imp,j}^{t+1,d})) \\ X_{Imp,j}^t & \text{Otherwise} \end{cases} \end{cases} \quad (18)$$

Each new subset $\overline{X_{Col,i}^{t+1}}$ or $\overline{X_{Imp,i}^{t+1}}$ feeds into MLP for training and testing purposes. Fig. 6 shows an overview of the FIS1 that addresses the FAGLVA's parametrisation issue. The

mechanism starts with five input entries. Each entry uses three membership functions (MFs) to map real values to descriptive terms {low, medium, high}. Fig. 7 shows MFs that follow smooth changes rather than sharp switching. In theory, MFs can handle uncertainty issues in EC-based FSs and help solve highly nonlinear, combinatorial and high-dimensional problems in a shorter time (Hancer, 2019).

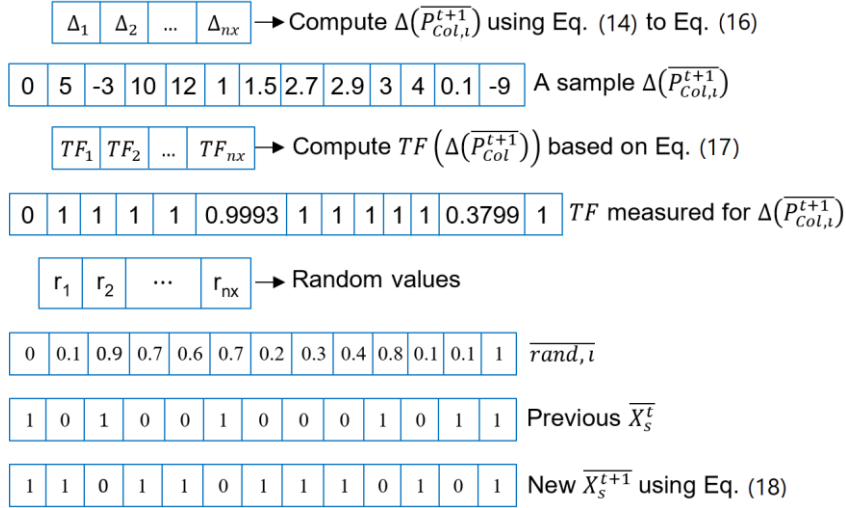


Fig. 5: A sample of the transformation of evolved solutions from the continuous decision space to the discrete binary decision space

$$\left\{ \begin{array}{l}
 NP_1(\overline{Xs}_{Col,t}^t) = \left| \frac{Power(\overline{Xs}_{Imp,J}^t) - Power(\overline{Xs}_{Col,t}^t)}{Power(\overline{Xs}_{Globalbest}^t)} \right| \\
 NP_2(\overline{Xs}_{Col,t}^t) = \left| \frac{Power(\overline{Xs}_{Ibest,Col,t}^t) - Power(\overline{Xs}_{Col,t}^t)}{Power(\overline{Xs}_{Globalbest}^t)} \right| \\
 NP_3(\overline{Xs}_{Imp,J}^t) = \left| \frac{Power(\overline{Xs}_{Globalbest}^t) - Power(\overline{Xs}_{Imp,J}^t)}{Power(\overline{Xs}_{Globalbest}^t)} \right| \\
 NP_4(\overline{Xs}_{Imp,J}^t) = \left| \frac{Power(\overline{Xs}_{Ibest,Imp,J}^t) - Power(\overline{Xs}_{Imp,J}^t)}{Power(\overline{Xs}_{Globalbest}^t)} \right| \\
 NIT = \frac{t}{Maximum\ Iteration}
 \end{array} \right. \quad (19)$$

The NP_1 measures how close the current candidate solution (i.e., colony) is to its associated imperialist. The NP_2 measures how close the candidate colony is to its best ever known experience. The NP_3 measures how close an imperialist is to the global best imperialist. The NP_4 measures how close an imperialist is to its best ever known experience. Fig. 8 shows defuzzifiers that map fuzzy linguistic terms to real numbers by calculating the centre of the areas under each curve.

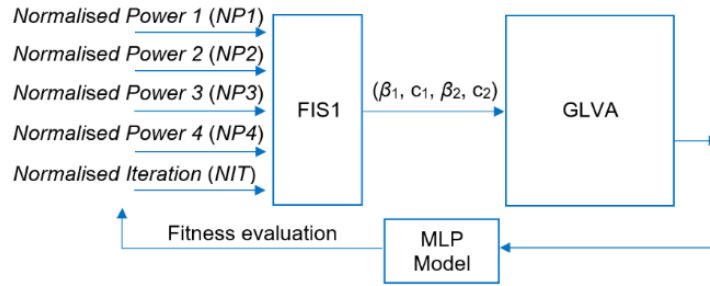


Fig. 6: An overview of the FIS1 introduced for the FAGLVA search component

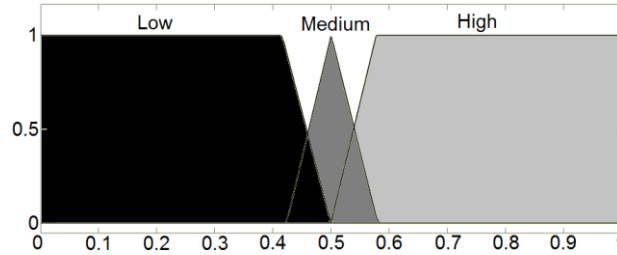


Fig. 7: Three MFs map real values of each input quantity to linguistic terms {low, medium and high}

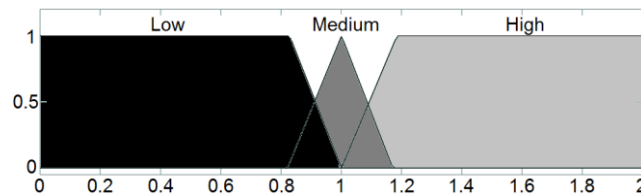


Fig. 8: Three MFs map linguistic terms {low, medium and high} to real values for each output parameter

Table 2: If-then statements for adapting the GLVA's parameters

# Rule	If (Status Indicators)					Then (Parameter Adaptation)			
	NP_1	NP_2	NP_3	NP_4	NIT	β_1	c_1	β_2	c_2
1	Low	Low	Low	Low	L or M	Low	Low	Low	Low
2	Low	Low	Low	High	L or M	Low	Low	Low	High
3	Low	Low	High	Low	L or M	Low	Low	High	Low
4	Low	Low	High	High	L or M	Low	Low	High	High
5	Low	High	Low	Low	L or M	Low	High	Low	Low
6	Low	High	Low	High	L or M	Low	High	Low	High
7	Low	High	High	Low	L or M	Low	High	High	Low
8	Low	High	High	High	L or M	Low	High	High	High
9	High	Low	Low	Low	L or M	High	Low	Low	Low
10	High	Low	Low	High	L or M	High	Low	Low	High
11	High	Low	High	Low	L or M	High	Low	High	Low
12	High	Low	High	High	L or M	High	Low	High	High
13	High	High	Low	Low	L or M	High	High	Low	Low
14	High	High	Low	High	L or M	High	High	Low	High
15	High	High	High	Low	L or M	High	High	High	Low
16	High	High	High	High	L or M	High	High	High	High
17	M	M	M	M	L or M	M	M	M	M
18	Any	Any	Any	Any	H	L	H	L	H

Table 2 lists a set of fuzzy rules designed for the GLVA. Rule 1, for instance, is designed to avoid premature convergence by assigning a low credence to the current convergence status and

biasing the framework towards more exploration tendency. The NP_1NP_4 are low and the NIT is low or medium. On the contrary, Rule 18 is designed to focus on exploitation rather than learning new information by giving a low credence to social learning coefficients β_1, β_2 and a high credence to cognitive learning coefficients c_1, c_2 . The NIT is high and there is not enough time for exploration.

3.1.3. Fuzzy adaptive universal diversity based velocity divergence (FAUDVD)

As represented by Eq. (20), each candidate colony learns from the best ever known experience of other colonies. Each imperialist learns from the best ever known experience of other imperialists. The global best imperialist learns from the best ever known experience of other imperialists. These learnings discourage premature convergence and are called universal diversity-based velocity divergence (UDVD). Similar to the previous component, the velocities update their positions. The TF maps these evolved positions to discrete binary values. Fig. 9 gives an overview of FIS2 that addresses the FAUDVD's parametrisation issue. Table 3 lists the fuzzy rules designed for UDVD.

$$\begin{cases} V_{Col,i}^{t+1} = w_1 \{V_{Col,i}^t + r_1 (P_{lbestCol,l}^t - P_{Col,i}^t)\}, \forall l \neq i \\ V_{Imp,j}^{t+1} = w_2 \{V_{Imp,j}^t + r_2 (P_{lbestImp,k}^t - P_{Imp,j}^t)\}, \forall k \neq j \\ V_{Globalbest}^{t+1} = w_3 \{V_{Globalbest}^t + r_3 (P_{lbestImp,k}^t - P_{Globalbest}^t)\} \end{cases}, \text{ if } r \leq PFAUDVD \quad (20)$$

A roulette-wheel selection procedure determines l -th colony and k -th imperialist:

$$\begin{cases} k = \text{Roulette Wheel Selection} \left(1 - \frac{\max_j Power_{imp,j} - Power_{imp,j}}{\sum_{j=1}^{\#total\ imperialists} (\max_j Power_{imp,j} - Power_{imp,j})} \right) \\ l = \text{Roulette Wheel Selection} \left(1 - \frac{\max_i Power_{Col,emp\ k} - Power_{Col,emp\ k}}{\sum_{i=1}^{\#colonies\ in\ emp\ k} (\max_i Power_{Col,emp\ k} - Power_{Col,emp\ k})} \right) \end{cases} \quad (21)$$

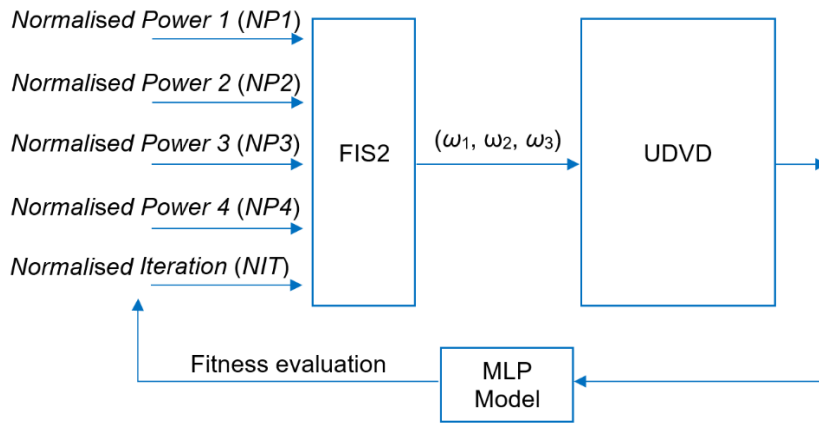


Fig. 9: An overview of the FIS2 introduced for the FAUDVD search component

Table 3: If-then statements for adapting parameters of the UDVD operator

If (status indicators)						Then (parameter adaptation)		
# Rule	NP_1	NP_2	NP_3	NP_4	NIT	ω_1	ω_2	ω_3
1	Low	Low	Low	Low	L or M	Low	Low	Low
2	Low	Low	Low	High	L or M	Low	Low	Low
3	Low	Low	High	Low	L or M	Low	High	Low
4	Low	Low	High	High	L or M	Low	High	Low
5	Low	High	Low	Low	L or M	Low	Low	Low
6	Low	High	Low	High	L or M	Low	Low	Low

7	Low	High	High	Low	L or M	Low	High	Low
8	Low	High	High	High	L or M	Low	High	Low
9	High	Low	Low	Low	L or M	High	Low	Low
10	High	Low	Low	High	L or M	High	Low	Low
11	High	Low	High	Low	L or M	High	High	Low
12	High	Low	High	High	L or M	High	High	Low
13	High	High	Low	Low	L or M	High	Low	Low
14	High	High	Low	High	L or M	High	Low	Low
15	High	High	High	Low	L or M	High	High	Low
16	High	High	High	High	L or M	High	High	High
17	M	M	M	M	L or M	M	M	M
18	Any	Any	Any	Any	High	Low	Low	Low

3.1.4. Fuzzy adaptive enhanced differential evolution based local search (FAEDELs)

A randomly selected colony, $\overline{P_{Col_{r,2,k}}^t}$, moves towards its imperialist, and moves in the reverse path of the worst colony. In the second relation, a randomly selected imperialist, $\overline{P_{Imp_{r,3,k}}^t}$, moves towards the global best imperialist, and it moves in the reverse path of the worst imperialist. Two randomly selected solutions make the movements stochastic. These movements model the mutation phase of enhanced differential evolution for local search (EDELs) and result in mutant vectors:

$$\begin{cases} \overline{V_{MutantCol,k}^{t+1}} = F_1 \cdot (\overline{P_{Col_{r,1,k}}^t} - \overline{P_{Col_{r,2,k}}^t}) + F_2 \cdot (\overline{P_{Imp_k}^t} - \overline{P_{Col_{r,3,k}}^t}) + F_3 \cdot (\overline{P_{Col_{r,3,k}}^t} - \overline{P_{wCol,k}^t}) \\ \overline{V_{MutantImp,k}^{t+1}} = F_4 \cdot (\overline{P_{Imp_{r,1,k}}^t} - \overline{P_{Imp_{r,2,k}}^t}) + F_5 \cdot (\overline{P_{Globalbest}^t} - \overline{P_{Imp_{r,3,k}}^t}) + F_6 \cdot (\overline{P_{Imp_{r,3,k}}^t} - \overline{P_{wImp}^t}) \text{ if } r \leq PFAEDELs \\ \overline{P_{Col_{r,1,2,3,k}}^t} \neq \overline{P_{wCol,k}^t}, \overline{P_{Imp_{r,1,2,3,k}}^t} \neq \overline{P_{wImp}^t} \end{cases} \quad (22)$$

Eq. (22) gives a good chance to randomly selected solutions in each empire and enables the framework to locate more optimality. F_i are scaling factors. Next, the mutants embed with randomly selected solutions; this is called the crossover phase, and it results in trial vectors:

$$\begin{cases} V_{TrialCol}^{t+1}{}^d = \begin{cases} V_{MutantCol}^{t+1}{}^d, & \text{if } rand() \leq PFAEDELs \\ V_{Col_{r,3}}^t{}^m, & \text{Otherwise} \end{cases} \\ V_{TrialImp}^{t+1}{}^d = \begin{cases} V_{MutantImp}^{t+1}{}^d, & \text{if } rand() \leq PFAEDELs \\ V_{Imp_{r,3}}^t{}^m, & \text{Otherwise} \end{cases} \end{cases} ; d = rand \text{ integer } \{1, \dots, n_x\} \quad (23)$$

$$\begin{cases} \overline{P_{TrialCol}^{t+1}} = \overline{P_{Col_{r,3}}^t} + \overline{V_{TrialCol}^{t+1}} \\ \overline{P_{TrialImp}^{t+1}} = \overline{P_{Imp_{r,3}}^t} + \overline{V_{TrialImp}^{t+1}} \end{cases} \quad (24)$$

$$\begin{cases} \Delta(\overline{P_{TrialCol}^{t+1}}) = \overline{P_{TrialCol}^{t+1}} - \overline{P_{Col_{r,3}}^t} \\ \Delta(\overline{P_{TrialImp}^{t+1}}) = \overline{P_{TrialImp}^{t+1}} - \overline{P_{Imp_{r,3}}^t} \end{cases} \quad (25)$$

$$\begin{cases} X_{S_{TrialCol}}^{t+1} = \begin{cases} Not(X_{S_{Col_{r3}}^t}) & \text{if } rand < TF(\Delta(P_{TrialCol}^{t+1})) \\ X_{S_{Col_{r3}}^t} & \text{Otherwise} \end{cases} \\ X_{S_{Triallmp}}^{t+1} = \begin{cases} Not(X_{S_{Imp_{r3}}^t}) & \text{if } rand < TF(\Delta(P_{Triallmp}^{t+1})) \\ X_{S_{Imp_{r3}}^t} & \text{Otherwise} \end{cases} \end{cases} \quad (26)$$

The selection compares the randomly selected solutions $\overline{X_{S_{Col_{r3}}^t}}$, $\overline{X_{S_{Imp_{r3}}^t}}$ with their related trials $\overline{X_{S_{TrialCol}}^{t+1}}$, $\overline{X_{S_{Triallmp}}^{t+1}}$ to select the better ones. Without controlling the parameters of mutation and crossover in the local search process, premature convergence occurs (Masoudi, Holling, & Wong, 2017).

$$\begin{cases} NP_5(\overline{X_{S_{Col_{r3}}^t}}) = \left| \frac{Power(\overline{X_{S_{Imp_{r3}}^t})} - Power(\overline{X_{S_{Col_{r3}}^t})}{Power(\overline{X_{S_{Globalbest}}^t})} \right| \\ NP_6(\overline{X_{S_{Col_{r3}}^t}}) = \left| \frac{Power(\overline{X_{S_{Col_{r3}}^t})} - Power(\overline{X_{S_{wCol}}^t})}{Power(\overline{X_{S_{Globalbest}}^t})} \right| \\ NP_7(\overline{X_{S_{Imp_{r3}}^t}}) = \left| \frac{Power(\overline{X_{S_{Globalbest}}^t}) - Power(\overline{X_{S_{Imp_{r3}}^t})}{Power(\overline{X_{S_{Globalbest}}^t})} \right| \\ NP_8(\overline{X_{S_{Imp_{r3}}^t}}) = \left| \frac{Power(\overline{X_{S_{Imp_{r3}}^t})} - Power(\overline{X_{S_{wImp}}^t})}{Power(\overline{X_{S_{Globalbest}}^t})} \right| \end{cases} \quad (27)$$

The NP_5 measures how close a randomly selected colony is to its associated imperialist. The NP_6 measures how close a randomly selected colony is to the weakest colony. The NP_7 measures how close a randomly selected imperialist is to the global best imperialist. The NP_8 measures how close a randomly selected imperialist is to the weakest imperialist. Fig. 10 gives an overview of the FIS3 that addresses the FAEDELs's parametrisation issue. Table 4 lists the fuzzy rules designed for EDELs.

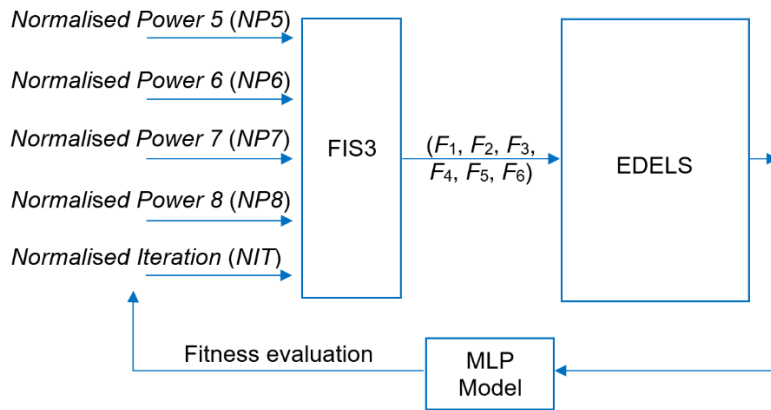


Fig. 10: An overview of the FIS3 introduced for the FAEDELs search component

Table 4: If-then statements for adapting parameters of the EDELs operator

If (status indicators)						Then (parameter adaptation)					
# Rule	NP_5	NP_6	NP_7	NP_8	NIT	F_1	F_2	F_3	F_4	F_5	F_6
1	Low	Low	Low	Low	L or M	High	High	Low	High	High	Low
2	Low	Low	Low	High	L or M	High	High	Low	Low	High	Low
3	Low	Low	High	Low	L or M	High	High	Low	High	Low	Low
4	Low	Low	High	High	L or M	High	High	Low	High	Low	High

5	Low	High	Low	Low	L or M	Low	High	High	High	High	Low
6	Low	High	Low	High	L or M	Low	High	High	Low	High	High
7	Low	High	High	Low	L or M	Low	High	High	High	Low	Low
8	Low	High	High	High	L or M	Low	High	High	High	Low	High
9	High	Low	Low	Low	L or M	High	Low	Low	High	High	Low
10	High	Low	Low	High	L or M	High	Low	Low	Low	High	High
11	High	Low	High	Low	L or M	Low	High	High	Low	High	High
12	High	Low	High	High	L or M	High	Low	Low	High	Low	High
13	High	High	Low	Low	L or M	High	Low	High	High	High	Low
14	High	High	Low	High	L or M	High	Low	High	Low	High	High
15	High	High	High	Low	L or M	High	Low	High	High	Low	Low
16	High	High	High	High	L or M	High	Low	High	High	Low	High
17	M	M	M	M	L or M	M	M	M	M	M	M
18	Any	Any	Any	Any	H	Low	High	Low	Low	High	Low

3.1.5. Fuzzy adaptive operator selection (FAOS)

Eq. (28) measures how much the global best imperialist has changed over the past time window, which is called the stagnation status. Lower stagnation is preferable:

$$Stagnation(\overline{Xs_{Globalbest}^{tw}}) = 1 - \frac{Max\ Power(\overline{Xs_{Globalbest}^{tw}}) - Min\ Power(\overline{Xs_{Globalbest}^{tw}})}{Max\ Power(\overline{Xs_{Globalbest}^{tw}})} \quad (28)$$

Fig. 11 gives an overview of the FIS4 that addresses the operator selection issue, known as FAOS. Table 5 lists the fuzzy rules designed to set the probability of applying each novel search component to the next time window:

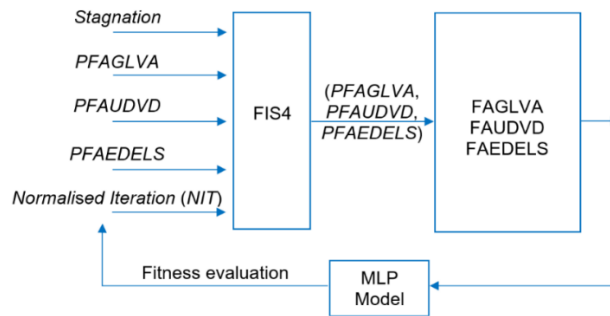


Fig. 11: An overview of the FIS4 introduced for the FAOS mechanism

Table 5: If-then statements for selecting operators

		If (status indicators)				Then (operator selection)			
# Rule	Stagnation	PFAGLVA	PFAUDVD	PFAEDELS	NIT	PFAGLVA	PFAUDVD	PFAEDELS	
1	Low	Low	Low	Low	L	Low	Low	Low	
2		Low	Low	High		Low	Low	High	
3		Low	High	Low		Low	High	Low	
4		Low	High	High		Low	High	High	
5		High	Low	Low		High	Low	Low	
6		High	Low	High		High	High	Low	High
7		High	High	Low		High	High	High	Low
8		High	High	High		High	High	High	High
9	High	Low	Low	Low		High	High	High	
10		Low	Low	High		High	High	Low	
11		Low	High	Low		High	Low	High	
12		Low	High	High		High	Low	Low	

13		High	Low	Low		Low	High	High
14		High	Low	High		Low	High	Low
15		High	High	Low		Low	Low	High
16		High	High	High		Low	Low	Low
17	Medium	M	M	M	M	M	M	M
18	Low	Low	Low	Low	H	High	High	High
19		Low	Low	High		High	High	Low
20		Low	High	Low		High	Low	High
21		Low	High	High		High	Low	Low
22		High	Low	Low		Low	High	High
23		High	Low	High		Low	High	Low
24		High	High	Low		Low	Low	High
25		High	High	High		Low	Low	Low
26	High	Low	Low	Low		Low	Low	Low
27		Low	Low	High		Low	Low	High
28		Low	High	Low		Low	High	Low
29		Low	High	High		Low	High	High
30		High	Low	Low		High	Low	Low
31		High	Low	High		High	Low	High
32		High	High	Low		High	High	Low
33		High	High	High		High	High	High

For example, rules 1–8 describe a good optimisation status because *Stagnation* is low. Therefore, the execution of novel search components continues as before. On the contrary, rules 9–16 refer to a bad optimisation status because *Stagnation* is high. Thus, the execution of novel search components will be the opposite of the previous state. Rules 18–33 are designed for exploitation rather than exploration and information sharing, as it refers to the end of the optimisation process.

3.2. Multi-objective fuzzy adaptive global learning local search universal diversity-based feature selection-MLP (MOFAGLSUD-based FS-MLP)

The framework extends our first proposal by introducing a new diversity-aware fitness evaluator based on the central moment concept—called spatial spread deviation associated with ranking (SSDR)—those accounts for the fitness of each solution in the same rank. Fig. 12 demonstrates an overview of the proposed framework. We first apply the domination rank process that finds the non-dominated feature subsets in the population of N_{Pop} solutions and assigns ranking values to each solution. Second, we design an archive at half the population’s size to keep a historical record of the first Pareto Front (PF). Third, we introduce SSDR fitness evaluator, which promotes diversity of Pareto Sets (PSs) in the decision space and their corresponding PFs in the objective space simultaneously. In the MOBFP problem, MOFAGLSUD-based feature selection extends MOFAEICA's penalised sigma index (Keivanian & Chiong, 2022) while using FAGLSUD’s search strategies.

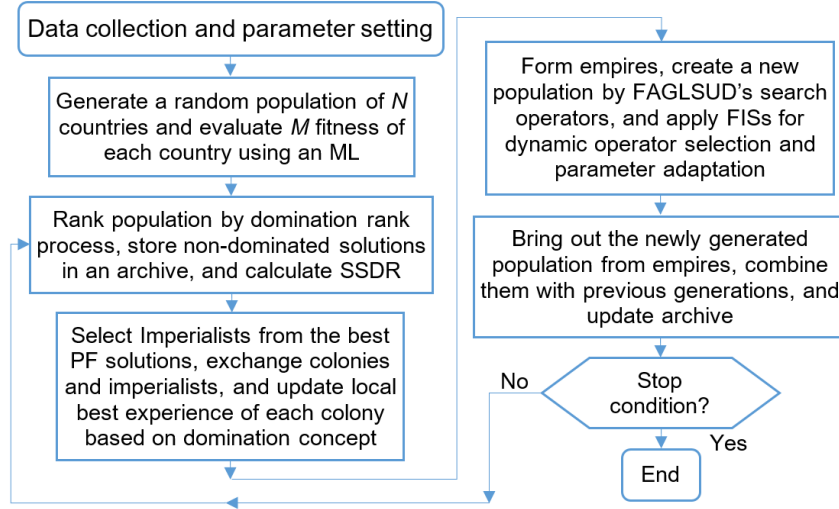


Fig. 12: The proposed MOFAGLSUD-based FS-ML

As a reference, Eq. (29) uses the difference between the maximum and minimum Euclidean distances between results in the objective space.

$$SSD_{i,rank(R)}^{OS} = \sqrt{\mu_{i,rank(R)}^{OS} + \sum_{j=2, i \neq j}^{k+1} \left(\frac{D_{max,rank(R)}^{OS} - D_{min,rank(R)}^{OS}}{D_{i,j,rank(R)}^{OS}} \right)} \quad (29)$$

where $D_{i,j,rank(R)}^{OS}$ measures the Euclidean distances in the OS and k refers to the neighbours.

Eq. (30) incorporates the number of conflicting objectives ($M=3$), as well as the rank values of solutions. In M –dimensional objective space, this capability helps avoid dense areas of similar objective values.

$$SSDR_{i,rank(R)}^{OS} = SSD_{i,rank(R)}^{OS} + (rank(R) - 1) \times M \quad (30)$$

To avoid dense areas in the $nVar$ –dimensional decision search space, Eq. (31) incorporates the number of design variables.

$$SSDR_{i,rank(R)}^{DS} = SSD_{i,rank(R)}^{DS} + (rank(R) - 1) \times nVar \quad (31)$$

The Euclidean distances are measured in a $nVar$ –dimensional decision space:

$$\begin{cases} \mu_{i,rank(R)}^{DS} = \frac{1}{(n_{rank(R)} - 1)} \sum_{j=1, j \neq i}^{n_{rank(R)}} \left(D_{i,j,rank(R)}^{DS} - (D_{max,rank(R)}^{DS} - D_{min,rank(R)}^{DS}) \right)^2 \\ D_{i,j,rank(R)}^{DS} = \sqrt{(P_{Sol,i}^1 - P_{Sol,j}^1)^2 + \dots + (P_{Sol,i}^{nVar} - P_{Sol,j}^{nVar})^2} \end{cases} \quad (32)$$

$SSDR_{i,rank(R)}^{OS}$ and $SSDR_{i,rank(R)}^{DS}$ are assigned to each solution on the same rank, which are high for solutions that have many surrounding solutions, forming dense areas, which is as an undesirable Pareto front approximation with a poor distribution. The following Eq. (33) measures the fitness of each solution (i.e., the power of each country):

$$Fitness_i \equiv Power_i = \frac{1}{SSDR_{i,rank(R)}^{OS} + SSDR_{i,rank(R)}^{DS}}, \quad \forall i: 1 \leq i \leq N_{Pop} \quad (33)$$

For the sake of complicity, the following relations are used as trial and tests:

$$\left\{ \begin{array}{l} \frac{1}{SSDR_{i,rank(R)}^{OS} \times SSDR_{i,rank(R)}^{DS}} \\ \frac{1}{\sqrt{SSDR_{i,rank(R)}^{OS} \times SSDR_{i,rank(R)}^{DS}}} \\ \frac{1}{\sqrt{SSDR_{i,rank(R)}^{OS}{}^2 + SSDR_{i,rank(R)}^{DS}{}^2}} \end{array} \right. \quad (34)$$

However, this obtains no better results.

4. EXPERIMENTS, RESULTS AND DISCUSSION

4.1. Experimental setup

The proposed framework was implemented using MATLAB 2019 on a 2.7 GHz Intel Core i5-7300U computation engine with 8 GB of RAM. The parameters were set as follows:

- In all evolutionary computation-based feature selection-ML models, the total population number was set to 10; the maximum number of iterations was set to 100; the position and velocity components of each solution were bound to zero to one and -12 to positive 12 , respectively. The number of imperialists and colonies was set to five and 15, respectively. The dimension of the decision space was set based on the number of features in the given dataset: say $d = 13$ for Dataset I and $d = 41$ for Dataset II. The time window tw was set as 10 iteration times, denoted as $tw = 10$.
- Liang, Xu et al. (2019) suggested $N_p/2$ as the size of the archive in the multi-objective evolutionary computation-based FS-ML models.
- The number of neurons in the input layer of the MLP model N_i was set to 13 and 41 for datasets I and II, respectively. The number of neurons in the output layer of the MLP model N_o was set to one for both datasets. The relation $N_h = \text{round}(\sqrt{N_i + N_o}) + c$ sets the number of neurons in the hidden layer (Shibata & Ikeda, 2009) and (Sheela & Deepa, 2013). Therefore, N_h was set to 10 and 15 and c was set to six and 8.5 for datasets I and II, respectively.
- In all comparisons, each metrics averaged five times to overcome uncertainty noise.

4.2. Data description

Datasets I and II came from the publicly available Johnson (1996b)'s dataset and NHANES that feature data on 252 and 862 male individuals from the US, respectively. For training and testing, 70% and 30% of cases were used, respectively. Table 6 lists the parameters of each dataset that formed the decision variables in the decision space:

Table 6: Dataset I (Johnson) and Dataset II (NHANES)

Dataset I		Dataset II		
X ₁	X ₂	Y ₁	Y ₂	Y ₃
Age (years)	Weight (lbs)	Segmented neutrophils number	Basophils number	Lymphocyte number
X ₃	X ₄	Y ₄	Y ₅	Y ₆
Height (inches)	Neck (cm)	Monocyte number	Eosinophils number	Red cell count SI
X ₅	X ₆	Y ₇	Y ₈	Y ₉
Chest (cm)	Abdomen (cm)	Haemoglobin	Haematocrit	MCV (Mean cell volume)
X ₇	X ₈	Y ₁₀	Y ₁₁	Y ₁₂
Hip (cm)	Thigh (cm)	MCH	MCHC	RDW
X ₉	X ₁₀	Y ₁₃	Y ₁₄	Y ₁₅
Knee (cm)	Ankle (cm)	Platelet #	MPV	SNA (sodium)
X ₁₁	X ₁₂	Y ₁₆	Y ₁₇	Y ₁₈

Biceps (cm)	Forearm (cm)	SK (Potassium)	SCL	SCA
X13		Y19	Y20	Y21
Wrist (cm)	SP (Phosphorus)	STB	BIC	
	Y22	Y23	Y24	
	GLU	Iron	LDH	
	Y25	Y26	Y27	
	Protein (STP)	SUA	SAL	
	Y28	Y29	Y30	
	TRI	BUN (Blood urea nitrogen)	CRP	
	Y31	Y32	Y33	
	SCR	STC (Cholesterol)	AST	
	Y34	Y35	Y36	
	ALT	GGT	ALP(alkaline phosphatase)	
	Y37	Y38	Y39	
	Weight (kg)	HT (Standing height)	Waist (cm)	
	Y40	Y41		
	Age	Full sample two-year MEC exam weight		

Body circumferences can measure the accumulation of fat in different parts of the body (Jindal, Baliyan, & Rana, 2018). For example, a high abdomen circumference signifies intensified abdominal fat. Clinical chemistry parameters can measure obesity through the blood (Fernández-Sánchez et al., 2011), (Ferenci, 2013). High hyperlipidaemia represents elevated or abnormal levels of lipids and/or lipoproteins in the blood. Fig. 13 depicts fats throughout the body organs and blood lipids.

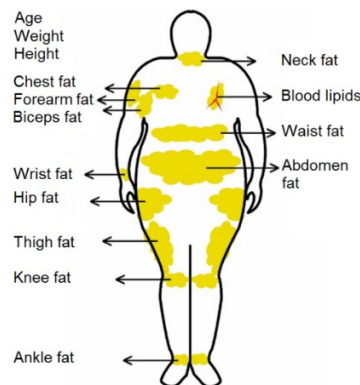


Fig. 13: A graphical view of fats in body organs and blood

4.3. Evaluation metrics

We applied four metrics—MAE, RMSE, MAPE and Theil’s inequality coefficient (TIC)—to evaluate accuracy. Lower values were preferable. We employed RMSE, the most commonly used criterion, to achieve accuracy in the multi-objective evolutionary computation-based FS-ML models. To quantify the volatility, we used STD. A lower value represented a higher stability. To evaluate the computational time and cost of the trained model, n_f measured the number of features selected. A lower value represented more computational time and cost savings for the trained model in body fat prediction.

4.4. Experiment I: Performance analysis of innovative search components

We investigated the role of each search component in terms of convergence speed and quality. Table 7 shows the best results highlighted in bold. The global learning local search universal diversity-based FS-MLP (GLSUD-based FS-MLP) lacked FISs, so the slowest convergence time

was obtained, validating the prominent role of FISs in tackling parametrisation and computational cost evaluation issues. The local search universal diversity-based FS-MLP (LSUD-based FS-MLP) lacked the FAGLVA component and produced results with the second slowest convergence time, revealing that without this exploitation component, the convergence rate becomes worse. The universal diversity-based FS-MLP (UD-based FS-MLP) had only universal diversity-based velocity divergence component, which produced the poorest results, indicating that using only exploration without exploitation and information sharing means the focus will be on diversification and the worst results will be obtained. Three novel fuzzy adaptive operators enabled the fuzzy adaptive global learning local search universal diversity-based FS-MLP (FAGLSUD-based FS-MLP) to escape from local optima and converge to the global best solution effectively.

Table 7: Effect of novel search components on the performance of the FAGLSUD-based FS-MLP

Dataset	Framework	Dimensionality		Accuracy				Volatility	Convergence time	Set of features
		r_f	n_f	MAE	RMS E	MAP E	TIC	STD		
I	FAGLSUD-based FS-MLP	38.46	5	3.1497	3.967	0.0118	0.0955	3.956	4.9066	X1, X6, X7, X12, X13
	GLSUD-based FS-MLP	38.46	5	3.3170	4.1344	0.0102	0.0994	4.1065	9.9313	X2, X4, X6, X9, X11
	LSUD-based FS-MLP	38.46	5	3.3377	4.1450	0.0132	0.0996	4.1274	8.0670	X4, X5, X6, X9, X13
	UD-based FS-MLP	53.85	7	3.3892	4.1518	0.0126	0.1000	4.1433	6.3271	X2, X3, X6, X7, X9, X12, X13
II	FAGLSUD-based FS-MLP	36.59	15	3.9936	5.1003	0.0040	0.1014	5.0902	11.2154	Y1, Y2, Y7, Y9, Y15, Y16, Y19, Y23, Y29, Y35, Y36, Y37, Y38, Y39, Y40
	GLSUD-based FS-MLP	41.46	17	4.2067	5.3935	0.0047	0.1074	5.3812	22.9160	Y2, Y5, Y7, Y8, Y17, Y19, Y23, Y24, Y25, Y28, Y29, Y32, Y33, Y35, Y36, Y38, Y39
	LSUD-based FS-MLP	39.02	16	4.0854	5.2585	0.0050	0.1049	5.2247	18.6130	Y5, Y6, Y12, Y13, Y17, Y18, Y25, Y27, Y28, Y29, Y33, Y36, Y37, Y38, Y39, Y41
	UD-based FS-MLP	46.34	19	4.2077	5.3363	0.0061	0.1069	5.3247	12.1548	Y3, Y7, Y8, Y9, Y11, Y14,

										Y15, Y16, Y17, Y20, Y29, Y30, Y32, Y33, Y34, Y36, Y37, Y38, Y39
--	--	--	--	--	--	--	--	--	--	---

4.5. Experiment II: Comparison of classical hybrid ML models and EC-based FS-ML models

We compared our FAGLSUD-based FS-MLP with several hybrid ML models and EC-based FS-ML models. The results in Table 8 reveal that our framework produced outstanding results in terms of dimensionality, accuracy and stability in most of the cases. Fig. 14 and Fig. 15 reveal more information about the prediction results. As is evident from the figures, our prediction values were very close to the target values and the errors were around zero. Thus, our FAGLSUD-based FS technique was effective for improving the performance of the MLP model.

Table 8: Predicting results of classical hybrid ML models and EC-based FS-ML models

Dataset	Frameworks	Dimensionality		Accuracy				Volatility	Set of features
		r _f	n _f	MAE	RMSE	MAPE	TIC	STD	
I	FAGLSUD-based FS-MLP	38.46	5	3.1497	3.967	0.0118	0.0955	3.956	X1, X6, X7, X12, X13
	FA-GL-BICA-based FS-MLP (F Keivanian et al., 2019)	38.46	5	3.2538	4.1125	0.0144	0.0993	4.1088	X2, X4, X6, X8, X10
	ICA-based FS-MLP (Mirhosseini & Nezamabadi-pour, 2018)	38.46	5	3.4077	4.2433	0.0167	0.1027	4.2331	X6, X8, X10, X12, X13
	FABGA-based FS-MLP (F Keivanian & N Mehrshad, 2015)	38.46	5	3.4086	4.2308	0.0162	0.1023	4.2044	X6, X8, X9, X11, X13
	PSO-based FS-MLP (Cervante et al., 2012)	38.46	5	3.3604	4.1607	0.0139	0.1003	4.1580	X2, X4, X6, X9, X11
	DE-based FS-MLP (He et al., 2009)	38.46	5	3.6377	4.5210	0.0185	0.1095	4.4936	X6, X9, X10, X12, X13
	MR-MARS (Shao, Hou, & Chiu, 2014)	46.15	6	3.5054	4.6384	0.0222	0.1130	-	X1, X2, X4, X6, X12, X13
	RF-IRE-SVM (Chiong, Fan, Hu, & Chiong, 2020)	-	-	3.5514	4.3391	-	-	4.3340	-
	DT-SVM (Uçar, Uçar, Köksal, & Daldal, 2021)	46.15	6	3.689	4.453	30.32	-	-	X3, X4, X5, X6, X7, X8
	FA-XGBoost (Fan et al., 2022)	46.15	6	3.433	4.248	0.949	-	4.188	-
	FAGLSUD-based FS-MLP	36.59	15	3.9936	5.1003	0.0040	0.1014	5.0902	Y1, Y2, Y7, Y9, Y15, Y16, Y19, Y23, Y29, Y35, Y36, Y37, Y38, Y39, Y40
	FA-GL-BICA-based FS-MLP (F Keivanian et al., 2019)	36.59	15	4.2861	5.4455	0.0065	0.1092	5.4330	Y2, Y5, Y6, Y12, Y13, Y17, Y18, Y19, Y21, Y22, Y28, Y31, Y36, Y39, Y40

II	ICA-based FS-MLP (Mirhosseini & Nezamabadi-pour, 2018)	39.02	16	4.1218	5.2438	0.0048	0.1045	5.2360	Y ₄ , Y ₅ , Y ₆ , Y ₈ , Y ₁₀ , Y ₁₃ , Y ₁₄ , Y ₁₆ , Y ₁₈ , Y ₂₀ , Y ₂₇ , Y ₂₈ , Y ₃₁ , Y ₃₂ , Y ₃₇ , Y ₃₉
	FABGA-based FS-MLP (F Keivanian & N Mehrshad, 2015)	39.02	16	4.2680	5.4425	0.0074	0.1096	5.3923	Y ₁ , Y ₃ , Y ₈ , Y ₉ , Y ₁₀ , Y ₁₆ , Y ₁₈ , Y ₂₀ , Y ₂₁ , Y ₂₇ , Y ₃₁ , Y ₃₃ , Y ₃₄ , Y ₃₆ , Y ₃₇ , Y ₃₉
	PSO-based FS-MLP (Cervante et al., 2012)	41.46	17	4.0238	5.1833	0.0056	0.1037	5.1687	Y ₅ , Y ₇ , Y ₉ , Y ₁₈ , Y ₁₉ , Y ₂₂ , Y ₂₅ , Y ₂₆ , Y ₂₇ , Y ₂₉ , Y ₃₁ , Y ₃₄ , Y ₃₆ , Y ₃₇ , Y ₃₉ , Y ₄₀ , Y ₄₁
	DE-based FS-MLP (He et al., 2009)	36.59	15	4.1825	5.3043	0.0052	0.1057	5.2508	Y ₁ , Y ₂ , Y ₄ , Y ₅ , Y ₉ , Y ₁₃ , Y ₁₄ , Y ₁₆ , Y ₂₂ , Y ₂₇ , Y ₃₀ , Y ₃₂ , Y ₃₇ , Y ₃₈ , Y ₃₉
	RF-IRE-SVM (Chiong et al., 2020)	-	-	4.4586	5.6426	-	-	5.6303	-
	FA-XGBoost (Fan et al., 2022)	29.27	12	4.169	5.276	0.946	-	5.255	-

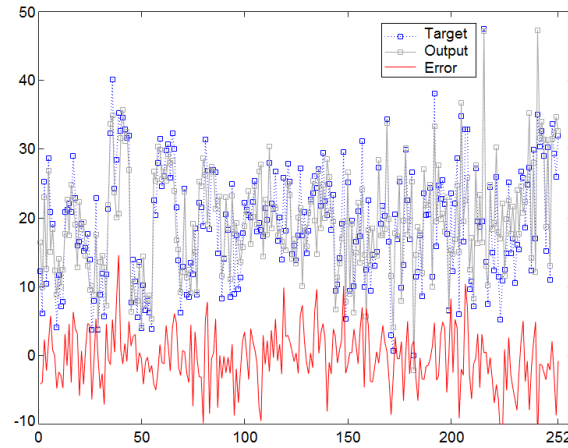


Fig. 14: All outputs of the FAGLSUD-based FS-MLP for 252 individuals using Dataset I

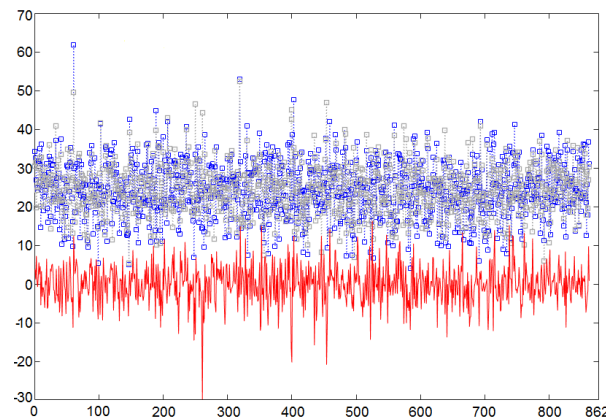


Fig. 15: All outputs of the FAGLSUD-based FS-MLP for 862 individuals using Dataset II

4.6. Experiment III: Comparison between MOEC-based FS-MLP

The convergence and distribution of the non-dominated Pareto fronts (PFs) achieved by four well-known multi-objective evolutionary feature selection (i.e., NSGA-II, MOPSO, MOICA, and multi-objective evolutionary algorithm with fuzzy logic based adaptive selection of operators

(FAME) (Santiago et al., 2019)-incorporated with the MLP machine learning model are visualised in the tri-objective space in Fig. 16 and Fig. 17. For a fair comparison, we have used the same machine learning model. As is evident from the figures, the MOFAGLSUD-based FS-MLP was able to find the best global Pareto sets associated with the evenly distributed global Pareto fronts along the objective space. However, the comparison frameworks were easily stuck in local Pareto sets and Pareto fronts without good distribution. A set of local and global Pareto sets and Pareto fronts found by five frameworks are listed in Table 9 and Table 10. As the tables show, the Pareto sets obtained by our approach dominated their counterparts. For example, X_{S1} dominated Y_{S1} ($X_{S1} > Y_{S1}$) because $F(X_{S1})$ was better than $F(Y_{S1})$ in terms of RMSE and STD. Thus, our method demonstrated superior performance in terms of the dominance and diversity quality of solutions and was able to escape from local Pareto optima.

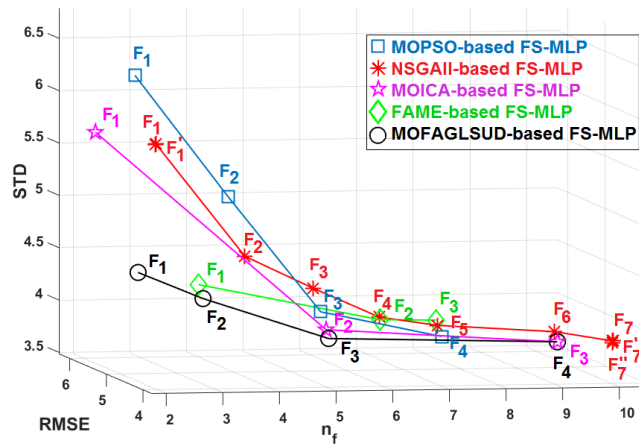


Fig. 16: Illustration of Pareto fronts found by the MOFAGLSUD-based FS-MLP and well-known multi-objective evolutionary computation-based feature selection-ML models using Dataset I

Table 9: Pareto Sets in the decision space and their related Pareto Fronts in the objective space found by the proposed MOFAGLSUD-based FS-MLP and well-known multi-objective evolutionary computation-based feature selection-ML models using Dataset I

Dataset	Frameworks	Objective Space				Decision Space	Domination
		PFs	n_f	RMSE	STD	PSs	
I	MOFAGLSUD-based FS-MLP	F ₁	2	4.531	4.526	X_{S1}	$X_{S1} > Y_{S1}$
		F ₂	3	4.304	4.303	X_{S2}	$X_{S2} > T_{S1} > W_{S1}$ or $W_{S2} > Z_{S1}$
		F ₃	5	3.967	3.956	X_{S3}	$X_{S3} > Y_{S2} > Z_{S3} > W_{S4}$
		F ₄	9	3.9055	3.9019	X_{S4}	$X_{S4} > Y_{S3} > W_{S7}$
	MOICA (Enayatifar et al., 2013)-based FS-MLP	F ₁	2	5.695	5.691	M_{S1}	$X_{S1} > M_{S1}$
		F ₂	5	4.036	4.03	M_{S2}	$X_{S3} > M_{S2} > Z_{S3} > W_{S4}$
		F ₃	9	3.906	3.902	M_{S3}	$X_{S4} > M_{S3} > W_{S7}$
	MOPSO (Coello et al., 2004)-based FS-MLP	F ₁	3	6.164	6.156	Z_{S1}	$X_{S2} > T_{S1} > W_{S1}$ or $W_{S2} > Z_{S1}$
		F ₂	4	5.159	5.137	Z_{S2}	$W_{S3} > Z_{S2}$
		F ₃	5	4.183	4.178	Z_{S3}	$X_{S3} > Y_{S2} > Z_{S3} > W_{S4}$
		F ₄	7	3.971	3.959	Z_{S4}	$Z_{S4} > W_{S6} > T_{S3}$
	NSGA-II (Deb et al., 2002)-based FS-MLP	F ₁	3	5.589	5.586	W_{S1}	$X_{S2} > T_{S1} > W_{S1}$ or $W_{S2} > Z_{S1}$
		F' ₁	3	5.616	5.575	W_{S2}	$X_{S2} > T_{S1} > W_{S1}$ or $W_{S2} > Z_{S1}$
		F ₂	4	4.709	4.638	W_{S3}	$W_{S3} > Z_{S2}$

	F ₃	5	4.381	4.373	W _{S4}	$X_{S3} > Y_{S2} > Z_{S3} > W_{S4}$
	F ₄	6	4.1318	4.1282	W _{S5}	$T_{S2} > W_{S5}$
	F ₅	7	4.083	4.048	W _{S6}	$Z_{S4} > W_{S6} > T_{S3}$
	F ₆	9	3.989	3.986	W _{S7}	$X_{S4} > Y_{S3} > W_{S7}$
	F ₇	10	3.934	3.899	W _{S8}	-
	F' ₇	10	3.955	3.878	W _{S9}	-
	F'' ₇	10	3.942	3.897	W _{S10}	-
FAME (Santiago et al., 2019)-based FS-MLP	F ₁	3	4.423	4.418	T _{S1}	$X_{S2} > T_{S1} > W_{S1} \text{ or } W_{S2} > Z_{S1}$
	F ₂	6	4.111	4.106	T _{S2}	$T_{S2} > W_{S5}$
	F ₃	7	4.13	4.092	T _{S3}	$Z_{S4} > W_{S6} > T_{S3}$

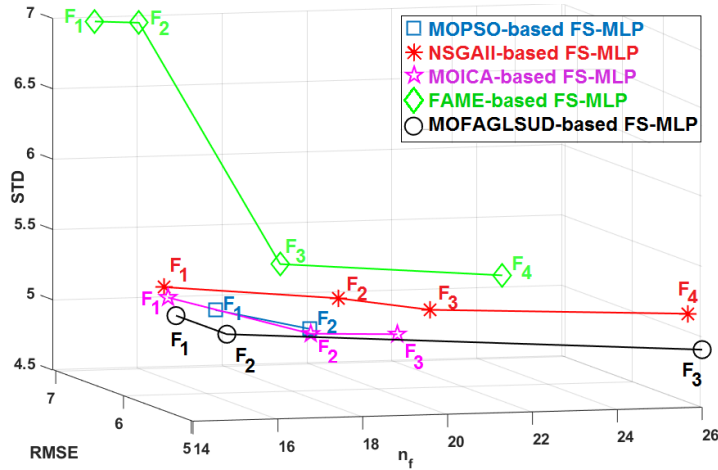


Fig. 17: Illustration of Pareto fronts found by the MOFAGLSUD-based FS-MLP and well-known multi-objective evolutionary computation-based feature selection-ML models using Dataset II

Table 10: Pareto Sets in the decision space and their related Pareto Fronts in the objective space found by the proposed MOFAGLSUD-based FS-MLP and well-known multi-objective evolutionary computation-based feature selection-ML models using Dataset II

Dataset	Frameworks	Objective Space				Decision Space	Domination
		PFs	n _f	RMSE	STD	PSs	
II	MOFAGLSUD-based FS-MLP	F ₁	14	5.225	5.209	Y _{S1}	$Y_{S1} > M_{S1} > W_{S1}$
		F ₂	15	5.1	5.09	Y _{S2}	$Y_{S2} > Z_{S1} > T_{S1}$
		F ₃	26	4.973	4.91	Y _{S3}	$Y_{S3} > W_{S4}$
	MOICA (Enayatifar et al., 2013)-based FS-MLP	F ₁	14	5.342	5.317	M _{S1}	$Y_{S1} > M_{S1} > W_{S1}$
		F ₂	17	5.114	5.074	M _{S2}	$Y_{S2} > Z_{S2} > T_{S3}$
		F ₃	19	5.089	5.059	M _{S3}	-
	MOPSO (Coello et al., 2004)-based FS-MLP	F ₁	15	5.267	5.233	Z _{S1}	$Y_{S2} > Z_{S1} > T_{S1}$
		F ₂	17	5.124	5.106	Z _{S2}	$Y_{S2} > Z_{S2} > T_{S3}$
	NSGA-II (Deb et al., 2002)-based FS-MLP	F ₁	14	5.395	5.381	W _{S1}	$Y_{S1} > Y_{S1} > W_{S1}$
		F ₂	18	5.331	5.28	W _{S2}	-
		F ₃	20	5.23	5.198	W _{S3}	-
		F ₄	26	5.18	5.129	W _{S4}	$Y_{S3} > W_{S4}$
	FAME (Santiago et al., 2019)-based FS-MLP	F ₁	15	7.05	6.969	T _{S1}	$Y_{S2} > Z_{S1} > T_{S1}$
		F ₂	16	7.025	6.956	T _{S2}	-
		F ₃	17	5.567	5.489	T _{S3}	$Y_{S2} > Z_{S2} > T_{S3}$
		F ₄	22	5.418	5.393	T _{S4}	-

4.7. Global best and global Pareto optimal solution(s)

Comprehensive experimental studies confirmed that our proposed FAGLSUD- and MOFAGLSUD-based FS-MLP were successful in dealing with the NP-hard, highly nonlinear, combinatorial, high-dimensional, multimodal and multi-objective body fat prediction problem. The FAGLSUD-based FS-MLP found the global best solution associated with the best trade-off between objectives. The MOFAGLSUD-based FS-MLP found global optimal Pareto sets corresponding to global optimal Pareto Fronts accurately instead of finding entire local optimal Pareto sets and Pareto fronts. Table 11 lists the global best and global optimal PSs that denote the most important parameters (i.e. body or blood measurements) contributing to the best prediction results. The latter produced trade-off solutions that enable user-preference flexibility. The parameters commonly found in the optimal solutions include the abdomen circumference from Dataset I and the potassium, phosphorus and gamma-glutamyl transferase measures, weight and waist circumference from Dataset II.

Table 11: The most important measurements in body fat prediction achieved by our proposed framework

Our Framework	Datasets	The most important parameters (the most relevant features)	
		Global optimal solution in the decision space	Global optimal Pareto sets in the decision space
FAGLSUD-based FS-MLP	I	$X_{S_{Globalbest}}$: {abdomen, hip, knee, ankle, wrist}	-
	II	$X_{S_{Globalbest}}$: {Segmented neutrophils, basophils, haemoglobin, MCV, SNA, SK, SP, Iron, BUN, GGT, ALP, weight, height, waist, age}	-
MOFAGLSUD-based FS-MLP	I	-	X_{S_1} : {chest, abdomen}
			X_{S_2} : {height, abdomen, biceps}
			X_{S_3} : {abdomen, hip, knee, ankle, wrist}
			X_{S_4} : {age, height, circumference of neck, abdomen, hip, ankle, biceps, forearm, wrist}
	II	-	X_{S_1} : {monocyte, platelet, SNA, SK, SP, SAL, CRP, SCR, STC (cholesterol), ALT, GGT, weight, waist, full sample two-year MEC exam weight}
			X_{S_2} : {segmented neutrophils, basophils, haemoglobin, MCV, SNA, SK, SP, Iron, BUN, GGT, ALP (alkaline), weight, height, waist, age}
X_{S_3} : {Segmented neutrophils, basophils, haemoglobin, MCV, MCH, MCHC, platelet, MPV, SK, SCL, SCA, SP, iron, protein (STP), SUA, TRI, BUN, SCR, ALT, GGT, ALP (alkaline), weight, height, waist, age, full sample two-year MEC exam weight}			

5. CONCLUSION, LIMITATIONS AND FUTURE WORK

This study treated body fat prediction as an NP-hard, combinatorial, high-dimensional, multimodal single and multi-objective optimisation problem. Although classical hybrid machine learning (ML) models (i.e., composed of feature selection and learning methods) showed superior performance in terms of accuracy and efficiency compared with solo ML models, they suffered

heavily in terms of computational cost and time with the increase of the feature space dataset. Evolutionary computation-based feature selection-ML (EC-based FS-ML) methods showed promising results by using global search, local search, and diversity promotion. However, because of the stochastic nature of a metaheuristic-based FS, there is no guarantee of finding the best optimal feature subset from combinations of feature subsets. Further, when providing high-dimensional datasets, these methods may become stuck in local optima, which is a more challenging issue—especially when multiple feature subsets in the decision space correspond to the identical or close prediction results in the objective space, presenting as a multimodality property in the optimisation process. To the best of our knowledge, these methods do not focus on prediction stability improvement and their evolutionary feature selection (EFS) module may require further analysis to determine optimum values for the control parameters and to control stochastic behaviour.

To address the aforementioned challenges, we first proposed the fuzzy adaptive evolutionary computation-based FS-ML framework, the FAGLSUD-based FS-MLP, to investigate the novel search components guided by fuzzy logic-based state observers to solve body fat prediction from a multimodal single-objective optimisation perspective (i.e., minimising a weighted sum of dimensionality: the number of features selected; accuracy: RMSE; and stability: STD). Experiment I investigated the role of FISs and search operators and revealed that fuzzy adaptive search components can effectively expedite the learning process and enhance the quality of prediction results. In Experiment II, the FAGLSUD-based FS-MLP efficiently outperformed the fuzzy adaptive evolutionary computation-based FS-ML models, such as the FA-GL-BICA-based FS-MLP, the ICA-based FS-MLP, the FABGA-based FS-MLP, the PSO-based FS-MLP, the DE-based FS-MLP, and hybrid ML models such as the MR-MARS, RF-IRE-SVM and DT-SVM, across three objectives (i.e., dimensionality: the number of features selected, accuracy: RMSE, and stability: STD).

We then extended our proposal to the multi-objective fuzzy adaptive evolutionary computation-based feature selection-machine learning (MOFAEC-based FS-ML), known as the MOFAGLSUD-based FS-MLP, by incorporating a domination rank process and a novel diversity-promotion index, spatial spread deviation associated with ranking (SSDR) developed based on the central moment concept, into the fitness of each solution lying in the same rank. Considering the distribution of solutions in the decision space and prediction results in the objective space, SSDR showed superior performance compared with its counterparts—crowded distance, spatial spread deviation (SSD), sigma index and grid concept integrated with Boltzmann relation—that were employed by the NSGA-II-, MOPSO-, MOICA-, and FAME-based FS-MLPs, respectively. In Experiment III, the MOFAGLSUD-based FS-MLP was compared to well-known multi-objective evolutionary computation algorithms incorporated into ML as multi-objective body fat prediction models and achieved better dominance and diversity by solving body fat prediction from a multimodal multi-objective optimisation perspective. Our approach found good distribution of global optimal Pareto sets (PSs) and their corresponding global optimal Pareto fronts (PFs), while its competitors easily became stuck in poor local optimal PSs and PFs.

Our framework and its multi-objective variant can provide a good reference point for people to determine their body fat percentage with easily accessible measurements. The comprehensive experiments conducted not only show that they have significantly better performance than other methods, but also confirm the usefulness of incorporating fuzzy adaptive evolutionary-based FS into the ML models. Our experiment used two case studies (Johnson: 252 individuals, each with 13 features, and NHANES: 862 individuals, each with 41 features), showing that considering more features does not necessarily enhance prediction performance because it does not increase the relevance, but instead increases the redundancy, the dimensionality, and the computation time.

We kept using the same learning model, the MLP, in our framework to assess the proposed fuzzy adaptive evolutionary computation-based FS modules. However, other learning models can

contribute to future research. We analysed males in both datasets; however, including gender (both male and female) as an explanatory variable (i.e., feature) could be a significant advantage for the next study, which is called gender-based body fat prediction. To develop software suitable for worldwide body fat prediction, databases from other countries are feasible options that could shed light on potential genetic differences between people of different ethnicities. The association between the percentage of body fat and cardiovascular risk factors, hypertension, dyslipidaemia and diabetes mellitus could create opportunities for future study, as both datasets used in this study did not include such disease information. Beyond body fat prediction, the framework could solve other health-related prediction problems using real-world datasets, such as diabetes or protein structure datasets. Despite achieving the best performance in three-objective body fat prediction, there is still room for further improvement of the framework devised in this study to solve prediction problems from the many-objective optimisation perspective—for example, minimising computational time and cost (i.e., reducing the ratio of features selected, known as dimensionality), RMSE (accuracy) and STD (stability) and maximising robustness against noise. The framework can be extended to solve prediction problems from a dynamic-optimisation view—for example, time-varying wind-speed prediction problems.

Compliance with Ethical Standards

Funding: The first author acknowledges the support of an Australian Government Research Training Program scholarship to carry out this research.

Conflicts of interest: The authors declare that they have no conflict of interest.

Ethical approval: This article does not contain any studies with human participants or animals performed by any of the authors.

Informed consent: Not applicable.

Data availability: All data included in this study are available from the first author and can also be found in the manuscript.

Code availability: All code included in this study are available from the first author upon reasonable request.

REFERENCES

- Alixandre, B. F. D. F., & Dorn, M. (2017). *D-BRKGA: a distributed biased random-key genetic algorithm*. Paper presented at the 2017 IEEE Congress on Evolutionary Computation (CEC).
- Azad, S. K., & Hasançebi, O. (2013). Upper bound strategy for metaheuristic based design optimization of steel frames. *Advances in Engineering Software*, 57, 19-32.
- Cervante, L., Xue, B., Zhang, M., & Shang, L. (2012). *Binary particle swarm optimisation for feature selection: A filter based approach*. Paper presented at the 2012 IEEE Congress on Evolutionary Computation.
- Chiong, R., Fan, Z., Hu, Z., & Chiong, F. (2020). Using an improved relative error support vector machine for body fat prediction. *Computer methods and programs in biomedicine*, 198, 105749.
- Coello, C. A. C., Pulido, G. T., & Lechuga, M. S. (2004). Handling multiple objectives with particle swarm optimization. *IEEE Transactions on Evolutionary Computation*, 8(3), 256-279.
- Deb, K., Pratap, A., Agarwal, S., & Meyarivan, T. (2002). A fast and elitist multiobjective genetic algorithm: NSGA-II. *IEEE Transactions on Evolutionary Computation*, 6(2), 182-197.
- DeGregory, K., Kuiper, P., DeSilvio, T., Pleuss, J., Miller, R., Roginski, J., . . . Heymsfield, S. (2018). A review of machine learning in obesity. *Obesity reviews*, 19(5), 668-685.

- Deurenberg, P., Yap, M., & Van Staveren, W. A. (1998). Body mass index and percent body fat: a meta analysis among different ethnic groups. *International journal of obesity*, 22(12), 1164-1171.
- Enayatifar, R., Yousefi, M., Abdullah, A. H., & Darus, A. N. (2013). MOICA: A novel multi-objective approach based on imperialist competitive algorithm. *Applied Mathematics and Computation*, 219(17), 8829-8841.
- Fan, Z., Chiong, R., Hu, Z., Keivanian, F., & Chiong, F. (2022). Body fat prediction through feature extraction based on anthropometric and laboratory measurements. *PloS one*, 17(2), e0263333.
- Ferenci, T. (2013). *Two applications of biostatistics in the analysis of pathophysiological processes*. PhD Thesis, Óbuda Univeristy, Budapest,
- Fernández-Sánchez, A., Madrigal-Santillán, E., Bautista, M., Esquivel-Soto, J., Morales-González, Á., Esquivel-Chirino, C., . . . Morales-González, J. A. (2011). Inflammation, oxidative stress, and obesity. *International journal of molecular sciences*, 12(5), 3117-3132.
- Freedman, D. S., Dietz, W. H., Srinivasan, S. R., & Berenson, G. S. (2009). Risk factors and adult body mass index among overweight children: the Bogalusa Heart Study. *Pediatrics*, 123(3), 750-757.
- Ghareb, A. S., Bakar, A. A., & Hamdan, A. R. (2016). Hybrid feature selection based on enhanced genetic algorithm for text categorization. *Expert Systems with Applications*, 49, 31-47.
- Ghasab, M. A. J., Khamis, S., Mohammad, F., & Fariman, H. J. (2015). Feature decision-making ant colony optimization system for an automated recognition of plant species. *Expert Systems with Applications*, 42(5), 2361-2370.
- Gonçalves, J. F., & Resende, M. G. (2011). Biased random-key genetic algorithms for combinatorial optimization. *Journal of Heuristics*, 17(5), 487-525.
- Goodarzi, M., Freitas, M. P., & Jensen, R. (2009). Ant colony optimization as a feature selection method in the QSAR modeling of anti-HIV-1 activities of 3-(3, 5-dimethylbenzyl) uracil derivatives using MLR, PLS and SVM regressions. *Chemometrics and intelligent laboratory systems*, 98(2), 123-129.
- Gunasundari, S., Janakiraman, S., & Meenambal, S. (2016). Velocity bounded boolean particle swarm optimization for improved feature selection in liver and kidney disease diagnosis. *Expert Systems with Applications*, 56, 28-47.
- Hancer, E. (2019). Differential evolution for feature selection: a fuzzy wrapper-filter approach. *Soft Computing*, 23(13), 5233-5248.
- He, X., Zhang, Q., Sun, N., & Dong, Y. (2009). *Feature selection with discrete binary differential evolution*. Paper presented at the 2009 International Conference on Artificial Intelligence and Computational Intelligence.
- Hussain, S. A., Cavus, N., & Sekeroglu, B. (2021). Hybrid machine learning model for body fat percentage prediction based on support vector regression and emotional artificial neural networks. *Applied Sciences*, 11(21), 9797.
- Jiang, S., Chin, K.-S., Wang, L., Qu, G., & Tsui, K. L. (2017). Modified genetic algorithm-based feature selection combined with pre-trained deep neural network for demand forecasting in outpatient department. *Expert Systems with Applications*, 82, 216-230.
- Jindal, K., Baliyan, N., & Rana, P. S. (2018). Obesity Prediction Using Ensemble Machine Learning Approaches. In *Recent Findings in Intelligent Computing Techniques* (pp. 355-362): Springer.
- Johnson, R. W. (1996a). Fitting percentage of body fat to simple body measurements. *Journal of Statistics Education*, 4(1).
- Johnson, R. W. (1996b). Fitting percentage of body fat to simple body measurements. *Journal of Statistics Education*, 4(1), 1-8.

- Keivanian, F., & Chiong, R. (2022). A novel hybrid fuzzy–metaheuristic approach for multimodal single and multi-objective optimization problems. *Expert Systems with Applications*, *195*, 116199.
- Keivanian, F., Chiong, R., & Hu, Z. (2019, 2019). *A Fuzzy Adaptive Binary Global Learning Colonization-MLP model for Body Fat Prediction*. the 3rd IEEE International Conference on Bio-Engineering for Smart Technologies (BioSMART 2019). France.
- Keivanian, F., Chiong, R., & Hu, Z. (2019). *A Fuzzy Adaptive Binary Global Learning Colonization-MLP model for Body Fat Prediction*. Paper presented at the 2019 3rd International Conference on Bio-engineering for Smart Technologies (BioSMART).
- Keivanian, F., & Mehrshad, N. (2015). *Intelligent feature subset selection with unspecified number for body fat prediction based on binary-GA and Fuzzy-Binary-GA*. Paper presented at the 2015 2nd International Conference on Pattern Recognition and Image Analysis (IPRIA).
- Keivanian, F., & Mehrshad, N. (2015). *Intelligent feature subset selection with unspecified number for body fat prediction based on binary-GA and Fuzzy-Binary-GA*. Paper presented at the Pattern Recognition and Image Analysis (IPRIA), 2015 2nd International Conference on.
- Khaled, A. A., & Hosseini, S. (2015). Fuzzy adaptive imperialist competitive algorithm for global optimization. *Neural Computing and Applications*, *26*, 813-825.
- Liang, J., Xu, W., Yue, C., Yu, K., Song, H., Crisalle, O. D., & Qu, B. (2019). Multimodal multiobjective optimization with differential evolution. *Swarm and Evolutionary Computation*, *44*, 1028-1059.
- Lin, S.-W., Ying, K.-C., Chen, S.-C., & Lee, Z.-J. (2008). Particle swarm optimization for parameter determination and feature selection of support vector machines. *Expert Systems with Applications*, *35*(4), 1817-1824.
- Liu, Y., Yen, G. G., & Gong, D. (2018). A multimodal multiobjective evolutionary algorithm using two-archive and recombination strategies. *IEEE transactions on evolutionary computation*, *23*(4), 660-674.
- Masoudi, E., Holling, H., & Wong, W. K. (2017). Application of imperialist competitive algorithm to find minimax and standardized maximin optimal designs. *Computational Statistics & Data Analysis*, *113*, 330-345.
- Mirhosseini, M., & Nezamabadi-pour, H. (2018). BICA: a binary imperialist competitive algorithm and its application in CBIR systems. *International Journal of Machine Learning and Cybernetics*, *9*(12), 2043-2057.
- Roque, L. A., Fontes, D. B., & Fontes, F. A. (2014). A hybrid biased random key genetic algorithm approach for the unit commitment problem. *Journal of Combinatorial Optimization*, *28*, 140-166.
- Safaei, M., Sundararajan, E. A., Driss, M., Boulila, W., & Shapi'i, A. (2021). A systematic literature review on obesity: Understanding the causes & consequences of obesity and reviewing various machine learning approaches used to predict obesity. *Computers in biology and medicine*, *136*, 104754.
- Saito, Y., Takahashi, O., Arioka, H., & Kobayashi, D. (2017). Associations between body fat variability and later onset of cardiovascular disease risk factors. *PloS one*, *12*(4), e0175057.
- Sakai, T., Demura, S., & Fujii, K. (2009). Validity of fat percentage evaluation for fat-thin judgement derived from standard weight in preschool children. *Sport Sciences for Health*, *5*, 105-112.
- Santiago, A., Dorronsoro, B., Nebro, A. J., Durillo, J. J., Castillo, O., & Fraire, H. J. (2019). A novel multi-objective evolutionary algorithm with fuzzy logic based adaptive selection of operators: FAME. *Information Sciences*, *471*, 233-251.
- Shao, Y. E. (2014). Body fat percentage prediction using intelligent hybrid approaches. *The Scientific World Journal*, 2014.

- Shao, Y. E., Hou, C.-D., & Chiu, C.-C. (2014). Hybrid intelligent modeling schemes for heart disease classification. *Applied Soft Computing*, 14, 47-52.
- Sheela, K. G., & Deepa, S. N. (2013). Review on methods to fix number of hidden neurons in neural networks. *Mathematical Problems in Engineering*, 2013.
- Shibata, K., & Ikeda, Y. (2009). *Effect of number of hidden neurons on learning in large-scale layered neural networks*. Paper presented at the 2009 ICCAS-SICE.
- Sikora, R., & Piramuthu, S. (2007). Framework for efficient feature selection in genetic algorithm based data mining. *European Journal of Operational Research*, 180(2), 723-737.
- Soyel, H., Tekguc, U., & Demirel, H. (2011). Application of NSGA-II to feature selection for facial expression recognition. *Computers & Electrical Engineering*, 37(6), 1232-1240.
- Svendsen, O. L., Haarbo, J., Heitmann, B. L., Gotfredsen, A., & Christiansen, C. (1991). Measurement of body fat in elderly subjects by dual-energy x-ray absorptiometry, bioelectrical impedance, and anthropometry. *The American journal of clinical nutrition*, 53(5), 1117-1123.
- Uçar, M. K., Uçar, Z., Köksal, F., & Daldal, N. (2021). Estimation of body fat percentage using hybrid machine learning algorithms. *Measurement*, 167, 108173.
- Wang, J., Thornton, J., Kolesnik, S., & Pierson Jr, R. (2000). Anthropometry in body composition: an overview. *Annals of the New York Academy of Sciences*, 904(1), 317-326.
- WHO. (2020). *WHO Reveals Leading Causes of Death and Disability Worldwide: 2000–2019*.
- Xue, B., Zhang, M., & Browne, W. N. (2014). Particle swarm optimisation for feature selection in classification: Novel initialisation and updating mechanisms. *Applied Soft Computing*, 18, 261-276.
- Zadeh, L. A. (1978). Fuzzy sets as a basis for a theory of possibility. *Fuzzy sets and systems*, 1(1), 3-28.